Fixed Point Theory and Algorithms for Sciences and Engineering

RESEARCH Open Access

Split monotone variational inclusion with errors for image-feature extraction with multiple-image blends problem

Pattanapong Tianchai[1*]

*Correspondence:
pattana@mju.ac.th
[1]Faculty of Science, Maejo University, Chiangmai 50290, Thailand

Abstract

In this paper, we introduce a new iterative forward–backward splitting algorithm with errors for solving the split monotone variational inclusion problem of the sum of two monotone operators in real Hilbert spaces. We suggest and analyze this method under some mild appropriate conditions imposed on the parameters such that another strong convergence theorem for this problem is obtained. We also apply our main result to image-feature extraction with the multiple-image blends problem, the split minimization problem, and the convex minimization problem, and provide numerical experiments to illustrate the convergence behavior and show the effectiveness of the sequence constructed by the inertial technique.

MSC: 47H05; 47H09; 47H20

Keywords: Split monotone variational inclusion problem; Convex minimization problem; Maximal monotone operator; Forward–backward method; Iterative shrinkage thresholding; Image-feature extraction; Multiple-image blends problem

1 Introduction

Let H_1 and H_2 be two real Hilbert spaces and $A : H_1 \to H_2$ be a bounded linear operator. Let $f_1 : H_1 \to H_1$ and $f_2 : H_2 \to H_2$ be two ψ_1 and ψ_2 inverse strongly monotone mappings, respectively, and $B_1 : H_1 \to 2^{H_1}$ and $B_2 : H_2 \to 2^{H_2}$ be two multivalued maximal monotone operators. The split monotone variational inclusion problem (SMVIP) is a fundamental problem in optimization theory, it can be applied to solve problems in many areas of science and applied science, engineering, economics, and medicine [1–9] such as image processing, machine learning, and modeling intensity-modulated radiation theory treatment planning [10–15], which is to find $x^* \in H_1$ such that

$$0 \in f_1(x^*) + B_1(x^*) \tag{1.1}$$

and such that

$$y^* = Ax^* \in H_2 \quad \text{solves } 0 \in f_2(y^*) + B_2(y^*), \tag{1.2}$$

and we will denote Ω the solution set of (1.1) and (1.2). That is

$$\Omega = \big\{x \in H_1 : x \text{ solves (1.1) and } y = Ax \text{ solves (1.2)}\big\}.$$

To solve SMVIP via the fixed-point theory, for $\lambda > 0$, we define the mappings $J_\lambda^{f_1,B_1} : H_1 \to H_1$ and $J_\lambda^{f_2,B_2} : H_2 \to H_2$ as follows:

$$J_\lambda^{f_1,B_1} = \underbrace{(I + \lambda B_1)^{-1}}_{\text{backward step}} \underbrace{(I - \lambda f_1)}_{\text{forward step}} = J_\lambda^{B_1}(I - \lambda f_1)$$

and

$$J_\lambda^{f_2,B_2} = (I + \lambda B_2)^{-1}(I - \lambda f_2) = J_\lambda^{B_2}(I - \lambda f_2),$$

where $J_\lambda^{B_1} = (I + \lambda B_1)^{-1}$ and $J_\lambda^{B_2} = (I + \lambda B_2)^{-1}$ are two resolvent operators of B_1 and B_2 for $\lambda > 0$, respectively. For $x \in H_1$ and $y = Ax \in H_2$, we see that

$$\begin{aligned} J_\lambda^{f_1,B_1}(x) = x \quad &\Leftrightarrow \quad x = (I + \lambda B_1)^{-1}\big(x - \lambda f_1(x)\big) \\ &\Leftrightarrow \quad x - \lambda f_1(x) \in x + \lambda B_1(x) \\ &\Leftrightarrow \quad 0 \in f_1(x) + B_1(x), \end{aligned}$$

and in the same way, we have

$$J_\lambda^{f_2,B_2}(y) = y \quad \Leftrightarrow \quad 0 \in f_2(y) + B_2(y).$$

This suggests the following iteration process to solve SMVIP, which is called the forward–backward splitting algorithm (FBSA) as follows: $x_1 \in H_1$ and

$$\begin{aligned} x_{n+1} &= J_\lambda^{f_1,B_1}\big(x_n + \gamma A^*\big(J_\lambda^{f_2,B_2} - I\big)Ax_n\big) \\ &= J_\lambda^{B_1}(I - \lambda f_1)\big(x_n + \gamma A^*\big(J_\lambda^{B_2}(I - \lambda f_2) - I\big)Ax_n\big), \end{aligned}$$

for all $n \in \mathbb{N}$, where $\lambda, \gamma > 0$. Moudafi [16] proved that the sequence $\{x_n\}$ of FBSA weakly converges to the solution of SMVIP under conditions $\gamma \in (0, \frac{1}{L})$ and $\lambda \in (0, 2\psi)$ such that $L = \|A\|^2$ and $\psi = \min\{\psi_1, \psi_2\}$.

Let $F_1 : H_1 \to \mathbb{R}$ and $F_2 : H_2 \to \mathbb{R}$ be two convex and differentiable functions and $G_1 : H_1 \to \mathbb{R} \cup \{\infty\}$ and $G_2 : H_2 \to \mathbb{R} \cup \{\infty\}$ be two convex and lower semicontinuous functions. The SMVIP can be reduced as follows.

If $f_1 = \nabla F_1, f_2 = \nabla F_2$ and $B_1 = \partial G_1, B_2 = \partial G_2$, where ∇F_1, ∇F_2 are two gradients of F_1, F_2, respectively, and ∂G_1, ∂G_2 are two subdifferentials of G_1, G_2, respectively, defined by

$$\partial G_1(x) = \big\{z \in H_1 : \langle y - x, z\rangle + G_1(x) \le G_1(y), \forall y \in H_1\big\}, \quad \forall x \in H_1,$$

and

$$\partial G_2(x) = \big\{z \in H_2 : \langle y - x, z\rangle + G_2(x) \le G_2(y), \forall y \in H_2\big\}, \quad \forall x \in H_2,$$

then, SMVIP is reduced to a split convex minimization problem (SCMP), which is to find $x^* \in H_1$ such that

$$F_1(x^*) + G_1(x^*) = \min_{x \in H_1}\{F_1(x) + G_1(x)\} \quad \Leftrightarrow \quad 0 \in \nabla F_1(x^*) + \partial G_1(x^*) \tag{1.3}$$

and such that $y^* = Ax^* \in H_2$ solves

$$F_2(y^*) + G_2(y^*) = \min_{y=Ax \in H_2}\{F_2(y) + G_2(y)\} \quad \Leftrightarrow \quad 0 \in \nabla F_2(y^*) + \partial G_2(y^*) \tag{1.4}$$

and we will denote by Γ the solution set of (1.3) and (1.4). That is,

$$\Gamma = \{x \in H_1 : x \text{ solves (1.3) and } y = Ax \text{ solves (1.4)}\}.$$

If $B_1 = \partial G_1 = \partial i_C$ and $B_2 = \partial G_2 = \partial i_Q$ are two subdifferentials of an indicator function of nonempty, closed, and convex subsets $C \subset H_1$ and $Q \subset H_2$, respectively, defined by

$$i_C(x) = \begin{cases} 0, & x \in C, \\ \infty, & x \notin C, \end{cases} \quad \text{and} \quad i_Q(x) = \begin{cases} 0, & x \in Q, \\ \infty, & x \notin Q, \end{cases}$$

then SMVIP is reduced to split a variational inequality problem (SVIP), which is to find $x^* \in C$ such that

$$\langle f_1(x^*), x - x^* \rangle \geq 0, \quad \forall x \in C$$

and $y^* = Ax^* \in Q$ such that

$$\langle f_2(y^*), y - y^* \rangle \geq 0, \quad \forall y \in Q.$$

If $f_1 = \nabla F_1, f_2 = \nabla F_2$, and $B_1 = B_2 = 0$ then SMVIP is reduced to a split feasibility problem (SFP), which is to find $x^* \in H_1$ such that

$$F_1(x^*) = \min_{x \in H_1} F_1(x) \quad \Leftrightarrow \quad 0 \in \nabla F_1(x^*)$$

and $y^* = Ax^* \in H_2$ such that

$$F_2(y^*) = \min_{y=Ax \in H_2} F_2(y) \quad \Leftrightarrow \quad 0 \in \nabla F_2(y^*).$$

If $f_2 = B_2 = 0$ then SMVIP is reduced to a monotone variational inclusion problem (MVIP), which is to find $x^* \in H_1$ such that

$$0 \in f_1(x^*) + B_1(x^*)$$

and when $f_1 = \nabla F_1$ and $B_1 = \partial G_1$, it can be reduced to a convex minimization problem (CMP), which is to find $x^* \in H_1$ such that

$$F_1(x^*) + G_1(x^*) = \min_{x \in H_1}\{F_1(x) + G_1(x)\} \quad \Leftrightarrow \quad 0 \in \nabla F_1(x^*) + \partial G_1(x^*).$$

Recall that the proximity operators $\operatorname{prox}_{\lambda G_1}$ of λG_1 and $\operatorname{prox}_{\eta G_2}$ of ηG_2 for $\lambda, \eta > 0$, respectively, are defined as follows:

$$\operatorname{prox}_{\lambda G_1}(x) = \operatorname*{Argmin}_{y \in H_1} \left\{ \lambda G_1(y) + \frac{1}{2}\|y - x\|_2^2 \right\}, \quad \forall x \in H_1$$

and

$$\operatorname{prox}_{\eta G_2}(x) = \operatorname*{Argmin}_{y \in H_2} \left\{ \eta G_2(y) + \frac{1}{2}\|y - x\|_2^2 \right\}, \quad \forall x \in H_2.$$

For $x \in H_1$, we see that

$$\begin{aligned} z = \operatorname{prox}_{\lambda G_1}(x) \quad &\Leftrightarrow \quad 0 \in \lambda \partial G_1(z) + z - x \\ &\Leftrightarrow \quad x \in (I + \lambda \partial G_1)(z) \\ &\Leftrightarrow \quad z = (I + \lambda \partial G_1)^{-1}(x) = J_\lambda^{\partial G_1}(x) \end{aligned}$$

and in the same way, for $y \in H_2$, we have

$$z = \operatorname{prox}_{\eta G_2}(y) \quad \Leftrightarrow \quad z = (I + \eta \partial G_2)^{-1}(y) = J_\eta^{\partial G_2}(y).$$

Therefore, SCMP is reduced to finding $x^* \in H_1$ such that

$$\begin{aligned} x^* \in \operatorname*{Argmin}_{x \in H_1} \{F_1(x) + G_1(x)\} \quad &\Leftrightarrow \quad 0 \in \nabla F_1(x^*) + \partial G_1(x^*) \\ &\Leftrightarrow \quad x^* = J_\lambda^{\nabla F_1, \partial G_1}(x^*) \\ &\Leftrightarrow \quad x^* = J_\lambda^{\partial G_1}(I - \lambda \nabla F_1)x^* = \operatorname{prox}_{\lambda G_1}(I - \lambda \nabla F_1)x^* \end{aligned}$$

and such that $y^* = Ax^* \in H_2$ solves

$$y^* \in \operatorname*{Argmin}_{y = Ax \in H_2} \{F_2(y) + G_2(y)\} \quad \Leftrightarrow \quad y^* = J_\eta^{\partial G_2}(I - \eta \nabla F_2)y^* = \operatorname{prox}_{\eta G_2}(I - \eta \nabla F_2)y^*.$$

Many researchers have proposed, analyzed, and modified FBSA for solving SMVIP and also for solving other problems such as the variational inclusion problem and related optimization problems (see also, [17–28]). The forward–backward splitting mapping with errors was introduced by Combettes and Wajs (see more details in [12]). Recently, Tianchai introduced a new iterative shrinkage thresholding algorithm (NISTA) with an error, based on the single forward–backward splitting mapping with an error for solving MVIP, and also solving the fixed-point set of nonexpansive mapping S (see, [29]), as follows: $x_0, x_1 \in H_1$ and

$$\begin{cases} y_n = x_n + \theta_n(x_n - x_{n-1}), \\ x_{n+1} = S(\alpha_n f(x_n) + (1 - \alpha_n) J_{\lambda_n}^{B_1}(y_n - \lambda_n f_1(y_n) + \varepsilon_n)), \end{cases}$$

for all $n \in \mathbb{N}$, and also introduced an improved fast iterative shrinkage thresholding algorithm (IFISTA) with an error for solving MVIP of the image-deblurring problem (see,

[30]) as follows: $x_0, x_1 \in H_1$ and

$$\begin{cases} z_n = x_n + \theta_n(x_n - x_{n-1}), \\ y_n = \alpha_n f(z_n) + (1-\alpha_n) J_{\lambda_n}^{B_1}(z_n - \lambda_n f_1(z_n) + \varepsilon_n), \\ x_{n+1} = J_{\lambda_n}^{B_1}(y_n - \lambda_n f_1(y_n) + \varepsilon_n), \end{cases}$$

for all $n \in \mathbb{N}$, where $J_{\lambda_n}^{B_1} = (I + \lambda_n B_1)^{-1}$ is a resolvent operator of B_1 for $\lambda_n > 0$, f is a contraction mapping, and $\{\alpha_n\} \subset (0,1)$, $\{\theta_n\} \subset [0,1)$, $\{\lambda_n\} \subset (0, 2\psi_1)$ and $\{\varepsilon_n\} \subset H_1$.

We introduce two forward–backward splitting mappings with errors $J_{\lambda_n,\varepsilon_n}^{f_1,B_1} : H_1 \to H_1$ and $J_{\eta_n,\xi_n}^{f_2,B_2} : H_2 \to H_2$ as follows:

$$J_{\lambda_n,\varepsilon_n}^{f_1,B_1} = (I + \lambda_n B_1)^{-1}\big((I - \lambda_n f_1) + \varepsilon_n\big) = J_{\lambda_n}^{B_1}\big((I - \lambda_n f_1) + \varepsilon_n\big)$$

and

$$J_{\eta_n,\xi_n}^{f_2,B_2} = (I + \eta_n B_2)^{-1}\big((I - \eta_n f_2) + \xi_n\big) = J_{\eta_n}^{B_2}\big((I - \eta_n f_2) + \xi_n\big),$$

for all $n \in \mathbb{N}$, where $J_{\lambda_n}^{B_1} = (I + \lambda_n B_1)^{-1}$ and $J_{\eta_n}^{B_2} = (I + \eta_n B_2)^{-1}$ are two resolvent operators of B_1 and B_2 for $\lambda_n, \eta_n > 0$, respectively, and $\{\varepsilon_n\} \subset H_1$, $\{\xi_n\} \subset H_2$. In this paper, we introduce the forward–backward splitting algorithm with errors (FBSA_Err) for solving SMVIP under some mild appropriate conditions on their parameters as follows: $x_0, x_1 \in H_1$ and

$$\begin{cases} z_n = x_n + \theta_n(x_n - x_{n-1}), \\ y_n = z_n + \gamma_n A^*(J_{\eta_n}^{B_2}((I - \eta_n f_2)Az_n + \xi_n) - Az_n), \\ x_{n+1} = \alpha_n f(y_n) + (1-\alpha_n) J_{\lambda_n}^{B_1}((I - \lambda_n f_1)y_n + \varepsilon_n), \end{cases}$$

for all $n \in \mathbb{N}$, where $\{\alpha_n\} \subset (0,1)$, $\{\theta_n\} \subset [0,1)$, $\{\lambda_n\} \subset (0, 2\psi_1]$, $\{\eta_n\} \subset (0, 2\psi_2]$ and $\{\gamma_n\} \subset (0, \frac{1}{L})$ such that $L = \|A\|^2$. Moreover, it can be applied to solve SCMP under some mild appropriate conditions on their parameters by letting $f_1 = \nabla F_1$, $f_2 = \nabla F_2$ and $B_1 = \partial G_1$, $B_2 = \partial G_2$ as follows: $x_0, x_1 \in H_1$ and

$$\begin{cases} z_n = x_n + \theta_n(x_n - x_{n-1}), \\ y_n = z_n + \gamma_n A^*(\operatorname{prox}_{\eta_n G_2}((I - \eta_n \nabla F_2)Az_n + \xi_n) - Az_n), \\ x_{n+1} = \alpha_n f(y_n) + (1-\alpha_n) \operatorname{prox}_{\lambda_n G_1}((I - \lambda_n \nabla F_1)y_n + \varepsilon_n), \end{cases}$$

for all $n \in \mathbb{N}$.

Our work is divided into several sections. In Sect. 2, some basic definitions and concepts are provided. In Sect. 3, the proof of the strong convergence theorem of FBSA_Err is presented. In Sect. 4, we propose the application of image restoration to the image-feature extraction with multiple-image blends problem, the split minimization problem, the convex minimization problem, and demonstrate the effectiveness of the sequence constructed by the inertial technique.

2 Preliminaries

Let C be a nonempty closed convex subset of a real Hilbert space H. We will use the notation: $\to$ to denote the strong convergence, $\rightharpoonup$ to denote the weak convergence, and $\mathrm{Fix}(T) = \{x : Tx = x\}$ to denote the fixed-point set of the mapping T.

Recall that the metric projection $P_C : H \to C$ is defined as follows: for each $x \in H$, $P_C x$ is the unique point in C satisfying

$$\|x - P_C x\| = \inf\{\|x - y\| : y \in C\}.$$

The operator $T : H \to H$ is called:

(i) monotone if

$$\langle x - y, Tx - Ty\rangle \geq 0, \quad \forall x, y \in H,$$

(ii) L-Lipschitzian with $L > 0$ if

$$\|Tx - Ty\| \leq L\|x - y\|, \quad \forall x, y \in H,$$

(iii) k-contraction if it is k-Lipschitzian with $k \in (0, 1)$,

(iv) nonexpansive if it is 1-Lipschitzian,

(v) firmly nonexpansive if

$$\|Tx - Ty\|^2 \leq \|x - y\|^2 - \|(I - T)x - (I - T)y\|^2, \quad \forall x, y \in H,$$

(vi) α-strongly monotone with $\alpha > 0$ if

$$\langle Tx - Ty, x - y\rangle \geq \alpha\|x - y\|^2, \quad \forall x, y \in H,$$

(vii) α-inverse strongly monotone with $\alpha > 0$ if

$$\langle Tx - Ty, x - y\rangle \geq \alpha\|Tx - Ty\|^2, \quad \forall x, y \in H.$$

Let B be a mapping of H into 2^H. The domain and the range of B are denoted by $D(B) = \{x \in H : Bx \neq \emptyset\}$ and $R(B) = \bigcup\{Bx : x \in D(B)\}$, respectively. The inverse of B, denoted by B^{-1}, is defined by $x \in B^{-1}y$ if and only if $y \in Bx$. A multivalued mapping B is said to be a monotone operator on H if $\langle x - y, u - v\rangle \geq 0$ for all $x, y \in D(B)$, $u \in Bx$ and $v \in By$. A monotone operator B on H is said to be maximal if its graph is not strictly contained in the graph of any other monotone operator on H. For a maximal monotone operator B on H and $r > 0$, we define the single-valued resolvent operator $J_r^B : H \to D(B)$ by $J_r^B = (I + rB)^{-1}$. It is well known that J_r^B is firmly nonexpansive and $\mathrm{Fix}(J_r^B) = B^{-1}(0)$.

We collect together some known lemmas that are the main tools in proving our result.

Lemma 2.1 ([31]) *Let C be a nonempty closed convex subset of a real Hilbert space H. Then,*

(i) $\|x \pm y\|^2 = \|x\|^2 \pm 2\langle x, y\rangle + \|y\|^2$, $\forall x, y \in H$,

(ii) $\|\lambda x + (1 - \lambda)y\|^2 = \lambda\|x\|^2 + (1 - \lambda)\|y\|^2 - \lambda(1 - \lambda)\|x - y\|^2$, $\forall x, y \in H, \lambda \in \mathbb{R}$,

(iii) $\langle x - P_C x, P_C x - y \rangle \geq 0$, $\forall x \in H, y \in C$,
(iv) $\|P_C x - P_C y\|^2 \leq \langle x - y, P_C x - P_C y \rangle$, $\forall x, y \in H$.

Lemma 2.2 ([32]) *Let H and K be two real Hilbert spaces and let $T : K \to K$ be a firmly nonexpansive mapping such that $\|(I - T)x\|$ is a convex function from K to $\overline{\mathbb{R}} = [-\infty, +\infty]$. Let $A : H \to K$ be a bounded linear operator and $f(x) = \frac{1}{2}\|(I - T)Ax\|^2$ for all $x \in H$. Then,*

(i) *f is convex and differentiable,*
(ii) *$\nabla f(x) = A^*(I - T)Ax$ for all $x \in H$ such that A^* denotes the adjoint of A,*
(iii) *f is weakly lower semicontinuous on H,*
(iv) *∇f is $\|A\|^2$-Lipschitzian.*

Lemma 2.3 ([32]) *Let H be a real Hilbert space and $T : H \to H$ be an operator. The following statements are equivalent*:
(i) *T is firmly nonexpansive,*
(ii) $\|Tx - Ty\|^2 \leq \langle x - y, Tx - Ty \rangle$, $\forall x, y \in H$,
(iii) *$I - T$ is firmly nonexpansive.*

Lemma 2.4 ([33]) *Let C be a nonempty closed convex subset of a real Hilbert space H. Let the mapping $A : C \to H$ be an α-inverse strongly monotone and $r > 0$ be a constant. Then, we have*

$$\big\|(I - rA)x - (I - rA)y\big\|^2 \leq \|x - y\|^2 - r(2\alpha - r)\|Ax - Ay\|^2$$

for all $x, y \in C$. In particular, if $0 < r \leq 2\alpha$ then $I - rA$ is nonexpansive.

Lemma 2.5 ([34] (Demiclosedness principle)) *Let C be a nonempty, closed, and convex subset of a real Hilbert space H and let $S : C \to C$ be a nonexpansive mapping with $\mathrm{Fix}(S) \neq \emptyset$. If the sequence $\{x_n\} \subset C$ converges weakly to x and the sequence $\{(I - S)x_n\}$ converges strongly to y. Then, $(I - S)x = y$; in particular, if $y = 0$ then $x \in \mathrm{Fix}(S)$.*

Lemma 2.6 ([35, 36]) *Let C be a nonempty, closed, and convex subset of a real Hilbert space H. Let $\{T_n\}$ and φ be two classes of nonexpansive mappings of C into itself such that*

$$\emptyset \neq \mathrm{Fix}(\varphi) = \bigcap_{n=0}^{\infty} \mathrm{Fix}(T_n).$$

Then, for any bounded sequence $\{z_n\} \subset C$, we have,

(i) *if $\lim_{n\to\infty} \|z_n - T_n z_n\| = 0$ then $\lim_{n\to\infty} \|z_n - Tz_n\| = 0$ for all $T \in \varphi$; which is called the NST-condition (I),*
(ii) *if $\lim_{n\to\infty} \|z_{n+1} - T_n z_n\| = 0$ then $\lim_{n\to\infty} \|z_n - T_m z_n\| = 0$ for all $m \in \mathbb{N} \cup \{0\}$; which is called the NST-condition (II).*

Lemma 2.7 ([37]) *Let $\{a_n\}$ and $\{c_n\}$ be sequences of nonnegative real numbers such that*

$$a_{n+1} \leq (1-\delta_n)a_n + b_n + c_n, \quad \forall n = 0, 1, 2, \ldots,$$

where $\{\delta_n\}$ is a sequence in $(0,1)$ and $\{b_n\}$ is a real sequence. Assume that $\sum_{n=0}^{\infty} c_n < \infty$. Then, the following results hold:

(i) *if $b_n \leq \delta_n M$ for some $M \geq 0$ then $\{a_n\}$ is a bounded sequence,*

(ii) *if $\sum_{n=0}^{\infty} \delta_n = \infty$ and $\limsup_{n\to\infty} b_n/\delta_n \leq 0$ then $\lim_{n\to\infty} a_n = 0$.*

Lemma 2.8 ([38]) *Assume that $\{s_n\}$ is a sequence of nonnegative real numbers such that*

$$s_{n+1} \leq (1-\mu_n)s_n + \mu_n\delta_n, \quad \forall n = 0, 1, 2, \ldots$$

and

$$s_{n+1} \leq s_n - \sigma_n + \rho_n, \quad \forall n = 0, 1, 2, \ldots,$$

where $\{\mu_n\}$ is a sequence in $(0,1)$, $\{\sigma_n\}$ is a sequence of nonnegative real numbers, and $\{\delta_n\}$, $\{\rho_n\}$ are real sequences such that

(i) $\sum_{n=0}^{\infty} \mu_n = \infty$,

(ii) $\lim_{n\to\infty} \rho_n = 0$,

(iii) *if $\lim_{k\to\infty} \sigma_{n_k} = 0$ then $\limsup_{k\to\infty} \delta_{n_k} \leq 0$ for any subsequence $\{n_k\}$ of $\{n\}$.*

Then, $\lim_{n\to\infty} s_n = 0$.

3 Main result

For solving the split monotone variational inclusion problem using the forward–backward splitting algorithm (with errors), we assume an initial condition (A), as follows:

$$\mathrm{Fix}(\mathcal{U}) = \bigcap_{n=1}^{\infty} \mathrm{Fix}(\mathcal{U}_n) \neq \emptyset \quad \text{and} \quad \mathrm{Fix}(\mathcal{V}) = \bigcap_{n=1}^{\infty} \mathrm{Fix}(\mathcal{V}_n) \neq \emptyset,$$

where $\mathcal{U} = J_{\lambda}^{B_1}(I - \lambda f_1)$, $\mathcal{V} = J_{\eta}^{B_2}(I - \eta f_2)$ and $\mathcal{U}_n = J_{\lambda_n}^{B_1}(I - \lambda_n f_1)$, $\mathcal{V}_n = J_{\eta_n}^{B_2}(I - \eta_n f_2)$ with $\lambda_n \to \lambda$ and $\eta_n \to \eta$ as $\to \infty$ such that f_1, f_2, B_1, B_2, and λ_n, η_n, λ, η are defined below.

Theorem 3.1 *Let H_1 and H_2 be two real Hilbert spaces and $A : H_1 \to H_2$ be a bounded linear operator. Let $f_1 : H_1 \to H_1$ and $f_2 : H_2 \to H_2$ be two ψ_1 and ψ_2 inverse strongly monotone mappings, respectively, and $B_1 : H_1 \to 2^{H_1}$ and $B_2 : H_2 \to 2^{H_2}$ be two multivalued maximal monotone operators. Let $f : H_1 \to H_1$ be a k-contraction mapping, and assume that Ω is nonempty and satisfies the condition (A). Let $x_0, x_1 \in H_1$ and $\{x_n\} \subset H_1$ be a sequence generated by*

$$\begin{cases} z_n = x_n + \theta_n(x_n - x_{n-1}), \\ y_n = z_n + \gamma_n A^*(J_{\eta_n}^{B_2}((I - \eta_n f_2)Az_n + \xi_n) - Az_n), \\ x_{n+1} = \alpha_n f(y_n) + (1-\alpha_n)J_{\lambda_n}^{B_1}((I - \lambda_n f_1)y_n + \varepsilon_n), \end{cases}$$

for all $n \in \mathbb{N}$, where $\{\alpha_n\} \subset (0,1)$, $\{\gamma_n\} \subset [a_1, b_1] \subset (0, \frac{1}{L})$ such that $L = \|A\|^2$, and $\{\lambda_n\} \subset [a_2, b_2] \subset (0, 2\psi_1]$, $\{\eta_n\} \subset [a_3, b_3] \subset (0, 2\psi_2]$ such that $\lambda_n \to \lambda$, $\eta_n \to \eta$ as $n \to \infty$, and $\{\varepsilon_n\} \subset H_1$, $\{\xi_n\} \subset H_2$, $\{\theta_n\} \subset [0,1)$ satisfy the following conditions:

(C1) $\lim_{n\to\infty}\alpha_n = 0$ *and* $\sum_{n=1}^{\infty}\alpha_n = \infty$,
(C2) $\lim_{n\to\infty}\frac{\|\varepsilon_n\|}{\alpha_n} = \lim_{n\to\infty}\frac{\|\xi_n\|}{\alpha_n} = 0$,
(C3) $\sum_{n=1}^{\infty}\|\varepsilon_n\| < \infty$ *and* $\sum_{n=1}^{\infty}\|\xi_n\| < \infty$,
(C4) $\lim_{n\to\infty}\frac{\theta_n}{\alpha_n}\|x_n - x_{n-1}\| = 0$,
then the sequence $\{x_n\}$ *converges strongly to a point* $x^* \in \Omega$, *where* $x^* = P_\Omega f(x^*)$.

Proof Selecting $p \in \Omega$ and fixing $n \in \mathbb{N}$, it follows that $p = J_{\lambda_n}^{B_1}(I - \lambda_n f_1)p$ and $Ap = J_{\eta_n}^{B_2}(I - \eta_n f_2)Ap$. First, we will show that $\{x_n\}$, $\{y_n\}$, and $\{z_n\}$ are bounded. Since,

$$\begin{aligned}\|z_n - p\| &= \big\|(x_n - p) + \theta_n(x_n - x_{n-1})\big\| \\ &\le \|x_n - p\| + \theta_n\|x_n - x_{n-1}\| \end{aligned} \tag{3.1}$$

and on the other hand, we have

$$\begin{aligned}&\gamma_n^2\|A^*\big(J_{\eta_n}^{B_2}\big((I - \eta_n f_2)Az_n + \xi_n\big) - Az_n\big)\|^2 \\ &\quad= \gamma_n^2\big\langle J_{\eta_n}^{B_2}\big((I - \eta_n f_2)Az_n + \xi_n\big) - Az_n, AA^*\big(J_{\eta_n}^{B_2}\big((I - \eta_n f_2)Az_n + \xi_n\big) - Az_n\big)\big\rangle \\ &\quad\le L\gamma_n^2\big\|J_{\eta_n}^{B_2}\big((I - \eta_n f_2)Az_n + \xi_n\big) - Az_n\big\|^2,\end{aligned}$$

and

$$\begin{aligned}&2\gamma_n\big\langle z_n - p, A^*\big(J_{\eta_n}^{B_2}\big((I - \eta_n f_2)Az_n + \xi_n\big) - Az_n\big)\big\rangle \\ &\quad= 2\gamma_n\big\langle Az_n - Ap, J_{\eta_n}^{B_2}\big((I - \eta_n f_2)Az_n + \xi_n\big) - Az_n\big\rangle \\ &\quad= 2\gamma_n\Big[\big\langle Az_n - Ap + J_{\eta_n}^{B_2}\big((I - \eta_n f_2)Az_n + \xi_n\big) - Az_n, J_{\eta_n}^{B_2}\big((I - \eta_n f_2)Az_n + \xi_n\big) - Az_n\big\rangle \\ &\qquad- \big\langle J_{\eta_n}^{B_2}\big((I - \eta_n f_2)Az_n + \xi_n\big) - Az_n, J_{\eta_n}^{B_2}\big((I - \eta_n f_2)Az_n + \xi_n\big) - Az_n\big\rangle\Big] \\ &\quad= 2\gamma_n\Bigg[\frac{1}{2}\Big(\big\|J_{\eta_n}^{B_2}\big((I - \eta_n f_2)Az_n + \xi_n\big) - Ap\big\|^2 + \big\|J_{\eta_n}^{B_2}\big((I - \eta_n f_2)Az_n + \xi_n\big) - Az_n\big\|^2 \\ &\qquad- \|Az_n - Ap\|^2\Big) - \big\|J_{\eta_n}^{B_2}\big((I - \eta_n f_2)Az_n + \xi_n\big) - Az_n\big\|^2\Bigg] \\ &\quad= -\gamma_n\big\|J_{\eta_n}^{B_2}\big((I - \eta_n f_2)Az_n + \xi_n\big) - Az_n\big\|^2 + \gamma_n\big\|J_{\eta_n}^{B_2}\big((I - \eta_n f_2)Az_n + \xi_n\big) - Ap\big\|^2 \\ &\qquad- \gamma_n\|Az_n - Ap\|^2.\end{aligned}$$

Therefore, it follows by nonexpansiveness of $J_{\eta_n}^{B_2}$ and $I - \eta_n f_2$ that

$$\begin{aligned}\|y_n - p\|^2 &= \big\|(z_n - p) + \gamma_n A^*\big(J_{\eta_n}^{B_2}\big((I - \eta_n f_2)Az_n + \xi_n\big) - Az_n\big)\big\|^2 \\ &= \|z_n - p\|^2 + \gamma_n^2\big\|A^*\big(J_{\eta_n}^{B_2}\big((I - \eta_n f_2)Az_n + \xi_n\big) - Az_n\big)\big\|^2 \\ &\quad+ 2\gamma_n\big\langle z_n - p, A^*\big(J_{\eta_n}^{B_2}\big((I - \eta_n f_2)Az_n + \xi_n\big) - Az_n\big)\big\rangle \\ &\le \|z_n - p\|^2 + L\gamma_n^2\big\|J_{\eta_n}^{B_2}\big((I - \eta_n f_2)Az_n + \xi_n\big) - Az_n\big\|^2 \\ &\quad- \gamma_n\big\|J_{\eta_n}^{B_2}\big((I - \eta_n f_2)Az_n + \xi_n\big) - Az_n\big\|^2 \\ &\quad+ \gamma_n\big\|J_{\eta_n}^{B_2}\big((I - \eta_n f_2)Az_n + \xi_n\big) - Ap\big\|^2 - \gamma_n\|Az_n - Ap\|^2 \\ &= \|z_n - p\|^2 - \gamma_n(1 - L\gamma_n)\big\|J_{\eta_n}^{B_2}\big((I - \eta_n f_2)Az_n + \xi_n\big) - Az_n\big\|^2\end{aligned}$$

$$
\begin{aligned}
&+ \gamma_n \left\| J_{\eta_n}^{B_2}\big((I-\eta_n f_2)Az_n + \xi_n\big) - J_{\eta_n}^{B_2}(I-\eta_n f_2)Ap \right\|^2 \\
&- \gamma_n \|Az_n - Ap\|^2 \\
&\le \|z_n - p\|^2 - \gamma_n(1-L\gamma_n)\left\| J_{\eta_n}^{B_2}\big((I-\eta_n f_2)Az_n + \xi_n\big) - Az_n \right\|^2 \\
&\quad + \gamma_n \left\| \big((I-\eta_n f_2)Az_n + \xi_n\big) - (I-\eta_n f_2)Ap \right\|^2 - \gamma_n \|Az_n - Ap\|^2 \\
&\le \|z_n - p\|^2 - \gamma_n(1-L\gamma_n)\left\| J_{\eta_n}^{B_2}\big((I-\eta_n f_2)Az_n + \xi_n\big) - Az_n \right\|^2 \\
&\quad + \gamma_n \big(\|Az_n - Ap\| + \|\xi_n\|\big)^2 - \gamma_n \|Az_n - Ap\|^2 \\
&= \|z_n - p\|^2 - \gamma_n(1-L\gamma_n)\left\| J_{\eta_n}^{B_2}\big((I-\eta_n f_2)Az_n + \xi_n\big) - Az_n \right\|^2 \\
&\quad + 2\gamma_n \|Az_n - Ap\|\|\xi_n\| + \gamma_n \|\xi_n\|^2 \\
&\le \|z_n - p\|^2 - \gamma_n(1-L\gamma_n)\left\| J_{\eta_n}^{B_2}\big((I-\eta_n f_2)Az_n + \xi_n\big) - Az_n \right\|^2 \\
&\quad + 2\left(\frac{1}{L}\right) L^{1/2}\|z_n - p\|\|\xi_n\| + \frac{1}{L}\|\xi_n\|^2 \\
&= \left(\|z_n - p\| + \frac{1}{\sqrt{L}}\|\xi_n\|\right)^2 \\
&\quad - \gamma_n(1-L\gamma_n)\left\| J_{\eta_n}^{B_2}\big((I-\eta_n f_2)Az_n + \xi_n\big) - Az_n \right\|^2. \qquad (3.2)
\end{aligned}
$$

This implies that

$$
\|y_n - p\| \le \|z_n - p\| + \frac{1}{\sqrt{L}}\|\xi_n\|. \qquad (3.3)
$$

Hence, by (3.1) and (3.3), and the nonexpansiveness of $J_{\lambda_n}^{B_1}$ and $I - \lambda_n f_1$, we have

$$
\begin{aligned}
\|x_{n+1} - p\| &= \left\| \alpha_n\big(f(y_n) - p\big) + (1-\alpha_n)\big(J_{\lambda_n}^{B_1}\big((I-\lambda_n f_1)y_n + \varepsilon_n\big) - p\big) \right\| \\
&\le \alpha_n\big(\left\|f(y_n) - f(p)\right\| + \left\|f(p) - p\right\|\big) \\
&\quad + (1-\alpha_n)\left\| J_{\lambda_n}^{B_1}\big((I-\lambda_n f_1)y_n + \varepsilon_n\big) - J_{\lambda_n}^{B_1}(I-\lambda_n f_1)p \right\| \\
&\le \alpha_n\big(k\|y_n - p\| + \left\|f(p) - p\right\|\big) \\
&\quad + (1-\alpha_n)\left\| \big((I-\lambda_n f_1)y_n + \varepsilon_n\big) - (I-\lambda_n f_1)p \right\| \\
&\le \alpha_n\big(k\|y_n - p\| + \left\|f(p) - p\right\|\big) + (1-\alpha_n)\big(\|y_n - p\| + \|\varepsilon_n\|\big) \\
&\le \big(1 - \alpha_n(1-k)\big)\|y_n - p\| + \alpha_n\left\|f(p) - p\right\| + \|\varepsilon_n\| \\
&\le \big(1 - \alpha_n(1-k)\big)\|z_n - p\| + \frac{1}{\sqrt{L}}\|\xi_n\| + \alpha_n\left\|f(p) - p\right\| + \|\varepsilon_n\| \\
&\le \big(1 - \alpha_n(1-k)\big)\|x_n - p\| + \alpha_n(1-k)\left[\frac{1}{1-k}\frac{\theta_n}{\alpha_n}\|x_n - x_{n-1}\|\right. \\
&\quad \left. + \frac{\|f(p) - p\|}{1-k}\right] + \left(\frac{1}{\sqrt{L}}\|\xi_n\| + \|\varepsilon_n\|\right).
\end{aligned}
$$

Hence, by conditions (C3) and (C4), and putting $M = \frac{1}{1-k}(\|f(p) - p\| + \sup_{n\in\mathbb{N}} \frac{\theta_n}{\alpha_n}\|x_n - x_{n-1}\|) \ge 0$ in Lemma 2.7 (i), we conclude that the sequence $\{\|x_n - p\|\}$ is bounded. That is, the sequence $\{x_n\}$ is bounded, and so is $\{z_n\}$. Moreover, by condition (C3), we obtain $\lim_{n\to\infty} \varepsilon_n = \lim_{n\to\infty} \xi_n = 0$, it follows that the sequence $\{y_n\}$ is also bounded.

Since, $P_\Omega f$ is a k-contraction on H_1, by Banach's contraction principle there exists a unique element $x^* \in H_1$ such that $x^* = P_\Omega f(x^*)$, that is $x^* \in \Omega$, it follows that $x^* = J_{\lambda_n}^{B_1}(I - \lambda_n f_1)x^*$ and $Ax^* = J_{\eta_n}^{B_2}(I - \eta_n f_2)Ax^*$. Now, we will show that $x_n \to x^*$ as $n \to \infty$. On the other hand, we have

$$\begin{aligned}
\|z_n - x^*\|^2 &= \langle z_n - x^*, z_n - x^* \rangle \\
&= \langle x_n + \theta_n(x_n - x_{n-1}) - x^*, z_n - x^* \rangle \\
&= \langle x_n - x^*, z_n - x^* \rangle + \theta_n \langle x_n - x_{n-1}, z_n - x^* \rangle \\
&\leq \|x_n - x^*\| \|z_n - x^*\| + \theta_n \|x_n - x_{n-1}\| \|z_n - x^*\| \\
&\leq \frac{1}{2}\big(\|x_n - x^*\|^2 + \|z_n - x^*\|^2\big) + \theta_n \|x_n - x_{n-1}\| \|z_n - x^*\|.
\end{aligned}$$

Therefore,

$$\|z_n - x^*\|^2 \leq \|x_n - x^*\|^2 + 2\theta_n \|x_n - x_{n-1}\| \|z_n - x^*\|. \tag{3.4}$$

Since,

$$\begin{aligned}
\|x_{n+1} - x^*\|^2 &= \langle \alpha_n f(y_n) + (1 - \alpha_n) J_{\lambda_n}^{B_1}\big((I - \lambda_n f_1)y_n + \varepsilon_n\big) - x^*, x_{n+1} - x^* \rangle \\
&= \langle \alpha_n \big(f(y_n) - x^*\big) + (1 - \alpha_n)\big(J_{\lambda_n}^{B_1}\big((I - \lambda_n f_1)y_n + \varepsilon_n\big) - x^*\big), x_{n+1} - x^* \rangle \\
&= \alpha_n \langle f(y_n) - f\big(x^*\big), x_{n+1} - x^* \rangle + \alpha_n \langle f\big(x^*\big) - x^*, x_{n+1} - x^* \rangle \\
&\quad + (1 - \alpha_n)\langle J_{\lambda_n}^{B_1}\big((I - \lambda_n f_1)y_n + \varepsilon_n\big) - x^*, x_{n+1} - x^* \rangle \\
&\leq \alpha_n k \|y_n - x^*\| \|x_{n+1} - x^*\| + \alpha_n \langle f\big(x^*\big) - x^*, x_{n+1} - x^* \rangle \\
&\quad + (1 - \alpha_n)\|J_{\lambda_n}^{B_1}\big((I - \lambda_n f_1)y_n + \varepsilon_n\big) - x^*\| \|x_{n+1} - x^*\| \\
&\leq \frac{1}{2}\alpha_n k\big(\|y_n - x^*\|^2 + \|x_{n+1} - x^*\|^2\big) + \alpha_n \langle f\big(x^*\big) - x^*, x_{n+1} - x^* \rangle \\
&\quad + \frac{1}{2}(1 - \alpha_n)\big(\|J_{\lambda_n}^{B_1}\big((I - \lambda_n f_1)y_n + \varepsilon_n\big) - x^*\|^2 + \|x_{n+1} - x^*\|^2\big),
\end{aligned}$$

it follows by (3.2) and (3.4), and the nonexpansiveness of $J_{\lambda_n}^{B_1}$ and $I - \lambda_n f_1$ that

$$\begin{aligned}
\|x_{n+1} - x^*\|^2 &\leq \frac{\alpha_n k}{1 + \alpha_n(1 - k)}\|y_n - x^*\|^2 + \frac{2\alpha_n}{1 + \alpha_n(1 - k)}\langle f\big(x^*\big) - x^*, x_{n+1} - x^* \rangle \\
&\quad + \frac{1 - \alpha_n}{1 + \alpha_n(1 - k)}\|J_{\lambda_n}^{B_1}\big((I - \lambda_n f_1)y_n + \varepsilon_n\big) - J_{\lambda_n}^{B_1}(I - \lambda_n f_1)x^*\|^2 \\
&\leq \alpha_n k\|y_n - x^*\|^2 + \frac{2\alpha_n}{1 + \alpha_n(1 - k)}\langle f\big(x^*\big) - x^*, x_{n+1} - x^* \rangle \\
&\quad + (1 - \alpha_n)\|\big((I - \lambda_n f_1)y_n + \varepsilon_n\big) - (I - \lambda_n f_1)x^*\|^2 \\
&\leq \alpha_n k\|y_n - x^*\|^2 + \frac{2\alpha_n}{1 + \alpha_n(1 - k)}\langle f\big(x^*\big) - x^*, x_{n+1} - x^* \rangle \\
&\quad + (1 - \alpha_n)\big(\|y_n - x^*\| + \|\varepsilon_n\|\big)^2 \\
&\leq \big(1 - \alpha_n(1 - k)\big)\|y_n - x^*\|^2 + \frac{2\alpha_n}{1 + \alpha_n(1 - k)}\langle f\big(x^*\big) - x^*, x_{n+1} - x^* \rangle
\end{aligned}$$

$$
\begin{aligned}
&+ 2\left\|y_n - x^*\right\| \|\varepsilon_n\| + \|\varepsilon_n\|^2 \\
&\leq \big(1-\alpha_n(1-k)\big)\left[\left(\left\|z_n - x^*\right\| + \frac{1}{\sqrt{L}}\|\xi_n\|\right)^2\right. \\
&\quad \left. - \gamma_n(1-L\gamma_n)\left\|J_{\eta_n}^{B_2}\big((I-\eta_n f_2)Az_n + \xi_n\big) - Az_n\right\|^2\right] \\
&\quad + \frac{2\alpha_n}{1+\alpha_n(1-k)}\big\langle f\big(x^*\big) - x^*, x_{n+1} - x^*\big\rangle + 2\left\|y_n - x^*\right\| \|\varepsilon_n\| + \|\varepsilon_n\|^2 \\
&\leq \big(1-\alpha_n(1-k)\big)\left[\left\|x_n - x^*\right\|^2 + 2\theta_n\|x_n - x_{n-1}\|\left\|z_n - x^*\right\|\right. \\
&\quad + \frac{2}{\sqrt{L}}\left\|z_n - x^*\right\|\|\xi_n\| + \frac{1}{L}\|\xi_n\|^2 \\
&\quad \left. - \gamma_n(1-L\gamma_n)\left\|J_{\eta_n}^{B_2}\big((I-\eta_n f_2)Az_n + \xi_n\big) - Az_n\right\|^2\right] \\
&\quad + \frac{2\alpha_n}{1+\alpha_n(1-k)}\big\langle f\big(x^*\big) - x^*, x_{n+1} - x^*\big\rangle + 2\left\|y_n - x^*\right\| \|\varepsilon_n\| + \|\varepsilon_n\|^2.
\end{aligned}
$$

Therefore,

$$
\begin{aligned}
\left\|x_{n+1} - x^*\right\|^2 \leq{}& \big(1-\alpha_n(1-k)\big)\left\|x_n - x^*\right\|^2 + \alpha_n(1-k)\left[\frac{2}{1-k}\frac{\theta_n}{\alpha_n}\|x_n - x_{n-1}\|\left\|z_n - x^*\right\|\right. \\
&+ \frac{2}{\sqrt{L}(1-k)}\frac{\|\xi_n\|}{\alpha_n}\left\|z_n - x^*\right\| + \frac{1}{L(1-k)}\frac{\|\xi_n\|}{\alpha_n}\|\xi_n\| \\
&+ \frac{2}{1-k}\frac{1}{1+\alpha_n(1-k)}\big\langle f\big(x^*\big) - x^*, x_{n+1} - x^*\big\rangle + \frac{2}{1-k}\frac{\|\varepsilon_n\|}{\alpha_n}\left\|y_n - x^*\right\| \\
&\left. + \frac{1}{1-k}\frac{\|\varepsilon_n\|}{\alpha_n}\|\varepsilon_n\|\right]
\end{aligned}
$$

and

$$
\begin{aligned}
&\|x_{n+1} - x^*\|^2 \\
&\quad \leq \left\|x_n - x^*\right\|^2 - \big(1-\alpha_n(1-k)\big)\gamma_n(1-L\gamma_n)\left\|J_{\eta_n}^{B_2}\big((I-\eta_n f_2)Az_n + \xi_n\big) - Az_n\right\|^2 \\
&\qquad + \left[2\alpha_n\frac{\theta_n}{\alpha_n}\|x_n - x_{n-1}\|\left\|z_n - x^*\right\| + \frac{2}{\sqrt{L}}\left\|z_n - x^*\right\|\|\xi_n\| + \frac{1}{L}\|\xi_n\|^2\right. \\
&\qquad \left. + 2\alpha_n\left\|f\big(x^*\big) - x^*\right\|\left\|x_{n+1} - x^*\right\| + 2\left\|y_n - x^*\right\|\|\varepsilon_n\| + \|\varepsilon_n\|^2\right],
\end{aligned}
$$

which are of the forms

$$
s_{n+1} \leq (1-\mu_n)s_n + \mu_n\delta_n
$$

and

$$
s_{n+1} \leq s_n - \sigma_n + \rho_n,
$$

respectively, where $s_n = \|x_n - x^*\|^2$, $\mu_n = \alpha_n(1-k)$, $\delta_n = \frac{2}{1-k}\frac{\theta_n}{\alpha_n}\|x_n - x_{n-1}\|\|z_n - x^*\| + \frac{2}{\sqrt{L}(1-k)}\frac{\|\xi_n\|}{\alpha_n}\|z_n - x^*\| + \frac{1}{L(1-k)}\frac{\|\xi_n\|}{\alpha_n}\|\xi_n\| + \frac{2}{1-k}\frac{1}{1+\alpha_n(1-k)}\langle f(x^*) - x^*, x_{n+1} - x^*\rangle + \frac{2}{1-k}\frac{\|\varepsilon_n\|}{\alpha_n}\|y_n -$

$x^*\| + \frac{1}{1-k}\frac{\|\varepsilon_n\|}{\alpha_n}\|\varepsilon_n\|$, $\sigma_n = (1-\alpha_n(1-k))\gamma_n(1-L\gamma_n)\|J^{B_2}_{\eta_n}((I-\eta_n f_2)Az_n + \xi_n) - Az_n\|^2$ and $\rho_n = 2\alpha_n\frac{\theta_n}{\alpha_n}\|x_n - x_{n-1}\|\|z_n - x^*\| + \frac{2}{\sqrt{L}}\|z_n - x^*\|\|\xi_n\| + \frac{1}{L}\|\xi_n\|^2 + 2\alpha_n\|f(x^*) - x^*\|\|x_{n+1} - x^*\| + 2\|y_n - x^*\|\|\varepsilon_n\| + \|\varepsilon_n\|^2$. Therefore, using conditions (C1), (C3), and (C4), we can check that all those sequences satisfy conditions (i) and (ii) in Lemma 2.8. To complete the proof, we verify that condition (iii) in Lemma 2.8 is satisfied. Let $\lim_{i\to\infty}\sigma_{n_i} = 0$. Then, by conditions (C1) and (C3), we have

$$\begin{aligned}&\lim_{i\to\infty}\left\|J^{B_2}_{\eta_{n_i}}\left((I-\eta_{n_i}f_2)Az_{n_i} + \xi_{n_i}\right) - Az_{n_i}\right\| = 0\\ &\lim_{i\to\infty}\left\|J^{B_2}_{\eta_{n_i}}(I-\eta_{n_i}f_2)Az_{n_i} - Az_{n_i}\right\| = 0.\end{aligned} \tag{3.5}$$

Consider a subsequence $\{z_{n_i}\}$ of $\{z_n\}$. As $\{z_n\}$ is bounded, so is $\{z_{n_i}\}$, and there exists a subsequence $\{z_{n_{i_j}}\}$ of $\{z_{n_i}\}$ that converges weakly to $x \in H_1$. Without loss of generality, we can assume that $z_{n_i} \rightharpoonup x$ as $i \to \infty$. It follows that $Az_{n_i} \rightharpoonup Ax$ as $i \to \infty$. Hence, by (3.5) and the demiclosedness at zero in Lemma 2.5, we obtain $y = Ax \in \mathrm{Fix}(J^{B_2}_{\eta}(I-\eta f_2))$, indeed also, $y = Ax \in \mathrm{Fix}(J^{B_2}_{\eta_{n_i}}(I-\eta_{n_i}f_2))$, that is $y = Ax$ solves $0 \in f_2(y) + B_2(y)$. Since,

$$\begin{aligned}\|y_{n_i} - x\| &\le \|z_{n_i} - x\| + \gamma_{n_i}\left\|A^*\left(J^{B_2}_{\eta_{n_i}}\left((I-\eta_{n_i}f_2)Az_{n_i} + \xi_{n_i}\right) - Az_{n_i}\right)\right\|\\ &\le \|z_{n_i} - x\| + \gamma_{n_i}\sqrt{L}\left\|J^{B_2}_{\eta_{n_i}}\left((I-\eta_{n_i}f_2)Az_{n_i} + \xi_{n_i}\right) - Az_{n_i}\right\|\end{aligned}$$

and

$$\begin{aligned}\|x_{n_i} - x\| &= \left\|(z_{n_i} - x) - \theta_{n_i}(x_{n_i} - x_{n_i-1})\right\|\\ &\le \|z_{n_i} - x\| + \alpha_{n_i}\frac{\theta_{n_i}}{\alpha_{n_i}}\|x_{n_i} - x_{n_i-1}\|,\end{aligned}$$

by conditions (C1), (C3), (C4), and (3.5), we obtain $y_{n_i} \rightharpoonup x$ and $x_{n_i} \rightharpoonup x$ as $i \to \infty$, it follows that $y_{n_i} - x_{n_i} \rightharpoonup 0$ as $i \to \infty$. Hence, by the nonexpansiveness of $J^{B_1}_{\lambda_{n_i}}$ and $I - \lambda_{n_i}f_1$, we obtain

$$\begin{aligned}&\|x_{n_i+1} - J^{B_1}_{\lambda_{n_i}}(I-\lambda_{n_i}f_1)x_{n_i}\|\\ &= \left\|\alpha_{n_i}f(y_{n_i}) + (1-\alpha_{n_i})J^{B_1}_{\lambda_{n_i}}\left((I-\lambda_{n_i}f_1)y_{n_i} + \varepsilon_{n_i}\right) - J^{B_1}_{\lambda_{n_i}}(I-\lambda_{n_i}f_1)x_{n_i}\right\|\\ &= \left\|\alpha_{n_i}\left(f(y_{n_i}) - J^{B_1}_{\lambda_{n_i}}(I-\lambda_{n_i}f_1)x_{n_i}\right)\right.\\ &\quad \left. + (1-\alpha_{n_i})\left(J^{B_1}_{\lambda_{n_i}}\left((I-\lambda_{n_i}f_1)y_{n_i} + \varepsilon_{n_i}\right) - J^{B_1}_{\lambda_{n_i}}(I-\lambda_{n_i}f_1)x_{n_i}\right)\right\|\\ &\le \alpha_{n_i}\left\|f(y_{n_i}) - J^{B_1}_{\lambda_{n_i}}(I-\lambda_{n_i}f_1)x_{n_i}\right\|\\ &\quad + (1-\alpha_{n_i})\left\|J^{B_1}_{\lambda_{n_i}}\left((I-\lambda_{n_i}f_1)y_{n_i} + \varepsilon_{n_i}\right) - J^{B_1}_{\lambda_{n_i}}(I-\lambda_{n_i}f_1)x_{n_i}\right\|\\ &\le \alpha_{n_i}\left\|f(y_{n_i}) - J^{B_1}_{\lambda_{n_i}}(I-\lambda_{n_i}f_1)x_{n_i}\right\|\\ &\quad + (1-\alpha_{n_i})\left\|\left((I-\lambda_{n_i}f_1)y_{n_i} + \varepsilon_{n_i}\right) - (I-\lambda_{n_i}f_1)x_{n_i}\right\|\\ &\le \alpha_{n_i}\left\|f(y_{n_i}) - J^{B_1}_{\lambda_{n_i}}(I-\lambda_{n_i}f_1)x_{n_i}\right\| + (1-\alpha_{n_i})\left(\|y_{n_i} - x_{n_i}\| + \|\varepsilon_{n_i}\|\right).\end{aligned}$$

Hence, by conditions (C1) and (C3), we have

$$\lim_{i\to\infty}\left\|x_{n_i+1} - J^{B_1}_{\lambda_{n_i}}(I-\lambda_{n_i}f_1)x_{n_i}\right\| = 0.$$

Therefore, by NST-condition (II) in Lemma 2.6, we obtain

$$\lim_{i\to\infty}\left\|x_{n_i}-J^{B_1}_{\lambda_{n_i}}(I-\lambda_{n_i}f_1)x_{n_i}\right\|=0.$$

Hence, by the demiclosedness at zero in Lemma 2.5 again, we obtain $x\in \mathrm{Fix}(J^{B_1}_{\lambda}(I-\lambda f_1))$, indeed also, $x\in \mathrm{Fix}(J^{B_1}_{\lambda_{n_i}}(I-\lambda_{n_i}f_1))$, that is x solves $0\in f_1(x)+B_1(x)$. It follows that $x=J^{B_1}_{\lambda_{n_i}}(I-\lambda_{n_i}f_1)x\in\Omega$. Since, by the nonexpansiveness of $J^{B_1}_{\lambda_{n_i}}$ and $I-\lambda_{n_i}f_1$, we have

$$\begin{aligned}
\|x_{n_i+1}-x_{n_i}\| &= \left\|\alpha_{n_i}\big(f(y_{n_i})-x_{n_i}\big)+(1-\alpha_{n_i})\big(J^{B_1}_{\lambda_{n_i}}\big((I-\lambda_{n_i}f_1)y_{n_i}+\varepsilon_{n_i}\big)-x_{n_i}\big)\right\|\\
&\le \alpha_{n_i}\left\|f(y_{n_i})-x_{n_i}\right\|+(1-\alpha_{n_i})\left\|J^{B_1}_{\lambda_{n_i}}\big((I-\lambda_{n_i}f_1)y_{n_i}+\varepsilon_{n_i}\big)-x_{n_i}\right\|\\
&\le \alpha_{n_i}\left\|f(y_{n_i})-x_{n_i}\right\|+(1-\alpha_{n_i})\Big(\left\|J^{B_1}_{\lambda_{n_i}}\big((I-\lambda_{n_i}f_1)y_{n_i}+\varepsilon_{n_i}\big)-x\right\|\\
&\quad +\|x_{n_i}-x\|\Big)\\
&= \alpha_{n_i}\left\|f(y_{n_i})-x_{n_i}\right\|+(1-\alpha_{n_i})\big(\|x_{n_i}-x\|\\
&\quad +\left\|J^{B_1}_{\lambda_{n_i}}\big((I-\lambda_{n_i}f_1)y_{n_i}+\varepsilon_{n_i}\big)-J^{B_1}_{\lambda_{n_i}}(I-\lambda_{n_i}f_1)x\right\|\big)\\
&\le \alpha_{n_i}\left\|f(y_{n_i})-x_{n_i}\right\|+(1-\alpha_{n_i})\big(\|x_{n_i}-x\|\\
&\quad +\left\|\big((I-\lambda_{n_i}f_1)y_{n_i}+\varepsilon_{n_i}\big)-(I-\lambda_{n_i}f_1)x\right\|\big)\\
&\le \alpha_{n_i}\left\|f(y_{n_i})-x_{n_i}\right\|+(1-\alpha_{n_i})\big(\|x_{n_i}-x\|+\|y_{n_i}-x\|+\|\varepsilon_{n_i}\|\big),
\end{aligned}$$

it follows by conditions (C1) and (C3) that $x_{n_i+1}-x_{n_i}\rightharpoonup 0$ as $i\to\infty$. Hence, by Lemma 2.1(iii) we obtain

$$\begin{aligned}
&\limsup_{i\to\infty}\big\langle f\big(x^*\big)-x^*,x_{n_i+1}-x^*\big\rangle\\
&\quad=\limsup_{i\to\infty}\big(\big\langle f\big(x^*\big)-x^*,x_{n_i+1}-x_{n_i}\big\rangle+\big\langle f\big(x^*\big)-x^*,x_{n_i}-x^*\big\rangle\big)\\
&\quad=\big\langle f\big(x^*\big)-x^*,x-x^*\big\rangle\le 0.
\end{aligned}$$

It follows by conditions (C1), (C2), (C3), and (C4) that $\limsup_{i\to\infty}\delta_{n_i}\le 0$. Hence, by Lemma 2.8, we conclude that $x_n\to x^*$ as $n\to\infty$. This completes the proof. □

Remark 3.2 Indeed, the parameter θ_n can be chosen as follows:

$$\theta_n=\begin{cases}\min\{\frac{\omega_n}{\|x_n-x_{n-1}\|},\alpha_n\} & \text{if } x_n\neq x_{n-1},\\ \alpha_n & \text{otherwise,}\end{cases}\qquad \forall n\in\mathbb{N},$$

and for the speed up of convergence, the parameter θ_n is often chosen as follows:

$$\theta_n=\begin{cases}\begin{cases}\sigma_n=\frac{1}{2^n}\text{ or}\\ \sigma_n=\frac{t_n-1}{t_{n+1}}\quad\text{such that } t_1=1 \text{ and } t_{n+1}=\frac{1+\sqrt{1+4t_n^2}}{2}\end{cases} & \text{if } n\le N,\\ \begin{cases}\min\{\frac{\omega_n}{\|x_n-x_{n-1}\|},\alpha_n\} & \text{if } x_n\neq x_{n-1},\\ \alpha_n & \text{otherwise,}\end{cases} & \text{otherwise,}\end{cases}\qquad \forall n\in\mathbb{N},$$

where $N\in\mathbb{N}$ and $\{\omega_n\}$ is a positive sequence such that $\omega_n=o(\alpha_n)$.

4 Applications and numerical examples

In this section, we give some applications of our result using FBSA_Err to the image-feature extraction with multiple-image blends problem, the split minimization problem and convex minimization problem.

4.1 Image-feature extraction with multiple-image blends problem

Let $F_1 : H_1 \to \mathbb{R}$ and $F_2 : H_2 \to \mathbb{R}$ be two convex and differentiable functions, $G_1 : H_1 \to \mathbb{R} \cup \{\infty\}$ and $G_2 : H_2 \to \mathbb{R} \cup \{\infty\}$ be two convex and lower semicontinuous functions such that the gradients ∇F_1 and ∇F_2 are $\frac{1}{\psi_1}$- and $\frac{1}{\psi_2}$-Lipschitz continuous functions, ∂G_1 and ∂G_2 are subdifferentials of G_1 and G_2, respectively. It is well known from [39] that $(1/\alpha)$-Lipschitz continuous functions are also α-inverse strongly monotones, that is, if ∇F_1 and ∇F_2 are $\frac{1}{\psi_1}$- and $\frac{1}{\psi_2}$-Lipschitz continuous functions, respectively, then both are also ψ_1 and ψ_2 inverse strongly monotones, respectively. Moreover, ∂G_1 and ∂G_2 are maximal monotones [40].

Putting $f_1 = \nabla F_1, f_2 = \nabla F_2$ and $B_1 = \partial G_1, B_2 = \partial G_2$ into Theorem 3.1, and we assume an initial condition (A^*) as follows:

$$\operatorname{Fix}(\mathcal{U}) = \bigcap_{n=1}^{\infty} \operatorname{Fix}(\mathcal{U}_n) \neq \emptyset \quad \text{and}$$

$$\operatorname{Fix}(\mathcal{V}) = \bigcap_{n=1}^{\infty} \operatorname{Fix}(\mathcal{V}_n) \neq \emptyset,$$

where $\mathcal{U} = \operatorname{prox}_{\lambda G_1}(I - \lambda \nabla F_1)$, $\mathcal{V} = \operatorname{prox}_{\eta G_2}(I - \eta \nabla F_2)$ and $\mathcal{U}_n = \operatorname{prox}_{\lambda_n G_1}(I - \lambda_n \nabla F_1)$, $\mathcal{V}_n = \operatorname{prox}_{\eta_n G_2}(I - \eta_n \nabla F_2)$ with $\lambda_n \to \lambda$ and $\eta_n \to \eta$ as $\to \infty$ such that F_1, F_2, G_1, G_2 and λ_n, η_n, λ, η are defined below, we obtain the following result.

Theorem 4.1 *Let H_1 and H_2 be two real Hilbert spaces and $A : H_1 \to H_2$ be a bounded linear operator. Let $F_1 : H_1 \to \mathbb{R}$ and $F_2 : H_2 \to \mathbb{R}$ be two convex and differentiable functions with $\frac{1}{\psi_1}$- and $\frac{1}{\psi_2}$-Lipschitz continuous gradients ∇F_1 and ∇F_2, respectively, and $G_1 : H_1 \to \mathbb{R}$ and $G_2 : H_2 \to \mathbb{R}$ be two convex and lower semicontinuous functions. Let $f : H_1 \to H_1$ be a k-contraction mapping, and assume that Γ is nonempty and satisfies the condition (A^*). Let $x_0, x_1 \in H_1$ and $\{x_n\} \subset H_1$ be a sequence generated by*

$$\begin{cases} z_n = x_n + \theta_n(x_n - x_{n-1}), \\ y_n = z_n + \gamma_n A^*(\operatorname{prox}_{\eta_n G_2}((I - \eta_n \nabla F_2)Az_n + \xi_n) - Az_n), \\ x_{n+1} = \alpha_n f(y_n) + (1 - \alpha_n)\operatorname{prox}_{\lambda_n G_1}((I - \lambda_n \nabla F_1)y_n + \varepsilon_n), \end{cases}$$

for all $n \in \mathbb{N}$, where $\{\alpha_n\} \subset (0,1)$, $\{\gamma_n\} \subset [a_1, b_1] \subset (0, \frac{1}{\|A\|^2})$, and $\{\lambda_n\} \subset [a_2, b_2] \subset (0, 2\psi_1]$, $\{\eta_n\} \subset [a_3, b_3] \subset (0, 2\psi_2]$ such that $\lambda_n \to \lambda$, $\eta_n \to \eta$ as $n \to \infty$, and $\{\varepsilon_n\} \subset H_1$, $\{\xi_n\} \subset H_2$, $\{\theta_n\} \subset [0,1)$ satisfy the following conditions:

(C1) $\lim_{n\to\infty} \alpha_n = 0$ *and* $\sum_{n=1}^{\infty} \alpha_n = \infty$,

(C2) $\lim_{n\to\infty} \frac{\|\varepsilon_n\|}{\alpha_n} = \lim_{n\to\infty} \frac{\|\xi_n\|}{\alpha_n} = 0$,

(C3) $\sum_{n=1}^{\infty} \|\varepsilon_n\| < \infty$ *and* $\sum_{n=1}^{\infty} \|\xi_n\| < \infty$,

(C4) $\lim_{n\to\infty} \frac{\theta_n}{\alpha_n} \|x_n - x_{n-1}\| = 0$,

then the sequence $\{x_n\}$ converges strongly to a point $x^* \in \Gamma$, where $x^* = P_\Gamma f(x^*)$.

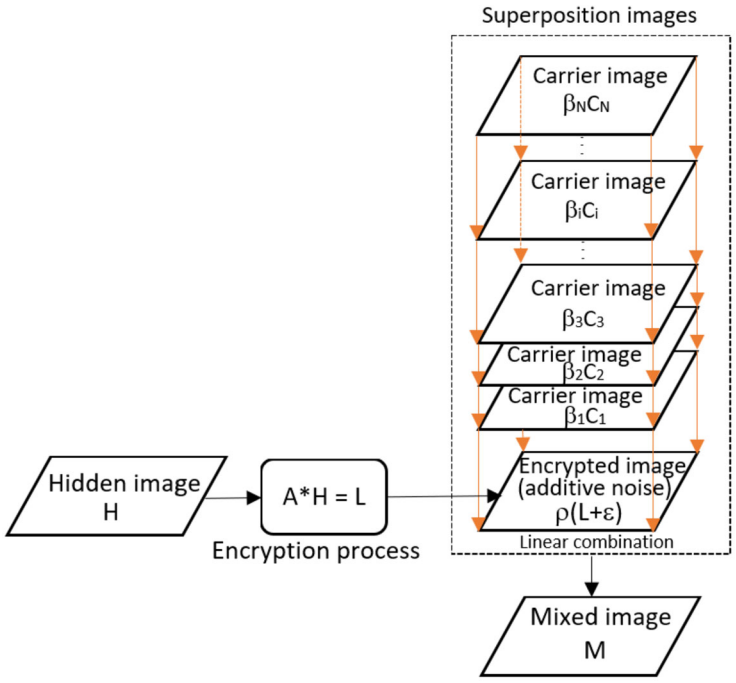

Figure 1 Image-encryption process and image-superposition process

We now propose the image-feature extraction with multiple-image blends using the fixed-point optimization algorithm in Theorem 4.1. The image information or the hidden image (messages) H went through a hybrid image-encryption system to the encrypted image L using the linear chaos-based method, and went through a digital image watermarking system using linear combination of superposition of carrier images $C_1, C_2, \ldots, C_N$ and the encrypted image with additive noise $L^\dagger$ to the mixed image M, see Fig. 1.

The discrete logistic chaotic map is defined as follows: $x_1 \in (0,1)$ and

$$x_{n+1} = \mu x_n(1 - x_n), \quad \forall n \in \mathbb{N},$$

where $0 < \mu \leq 4$, and when $3.57 \leq \mu \leq 4$, the unpredictability of the sequence $\{x_n\}$ is generated by logistic chaotic maps. We introduce the linear method for image encryption using logistic chaotic maps as follows:

$$A * x = L + \varepsilon, \tag{4.1}$$

where $A * x$ is Hadamard product (element-wise multiplication) of A and x such that $A \in \mathbb{R}^{m\times m}$ represents a known image-encryption operator (which is called the point-spread function: PSF) such that stacking the columns of A corresponding with a discrete logistic chaotic map $\{x_n\}_{n=1}^{m^2}$, and $L \in \mathbb{R}^{m\times m}$ is a known encrypted image, $\varepsilon \in \mathbb{R}^{m\times m}$ is an unknown white Gaussian noise, and $x \in \mathbb{R}^{m\times m}$ is an unknown image to be decrypted, the (estimated) image.

Let $C_1, C_2, \ldots, C_N \in \mathbb{R}^{m\times m}$ be N-carrier images, and $\{\mu_n\}_{n=1}^N \subset (0,1)$. We introduce the linear combination method for image mixing of superposition carrier images $C_1, C_2, \ldots,$

C_N, and the encrypted image with additive white Gaussian noise $L^\dagger = L + \varepsilon$ as follows:

$$\begin{aligned}
&M_1 = \mu_1 C_1 + (1-\mu_1)L^\dagger,\\
&M_2 = \mu_2 C_2 + (1-\mu_2)M_1,\\
&M_3 = \mu_3 C_3 + (1-\mu_3)M_2,\\
&\vdots\\
&M_N = \mu_N C_N + (1-\mu_N)M_{N-1},
\end{aligned}$$

where $M = M_N$, which is called the superimposed mixed image. For each $N \in \mathbb{N}$, it is clear that

$$\left(\prod_{i=1}^{N}(1-\mu_i)\right)L^\dagger = M - \sum_{i=1}^{N}\left[\left(\prod_{\substack{j=i+1\\ i\neq N}}^{N}(1-\mu_j)\right)\mu_i C_i\right],$$

$$\rho(A * x) = M - \sum_{i=1}^{N}\beta_i C_i, \tag{4.2}$$

where $\rho = \prod_{i=1}^{N}(1-\mu_i)$ and

$$\beta_i = \begin{cases} (\prod_{j=i+1}^{N}(1-\mu_j))\mu_i, & i \neq N,\\ \mu_i, & i = N. \end{cases}$$

For brevity, we use the notation Ax instead of $A * x$. In order to solve (4.1) and (4.2) of the solution set Γ using Theorem 4.1, we let $F_1(x) = \|Ax - L^\dagger\|_2^2$, $F_2(y) = \|\rho(y) - (M - \sum_{i=1}^{N}\beta_i C_i)\|_2^2$ and $G_1(x) = \kappa_1\|x\|_1$, $G_2(y) = \kappa_2\|y\|_1$ with $y = Ax \in \mathbb{R}^{m\times m}$ for all $x \in \mathbb{R}^{m\times m}$ such that $\kappa_1, \kappa_2 > 0$, and for $(x_1, x_2, \ldots, x_{m^2})^T \in \mathbb{R}^{m^2}$ corresponding to stacking the columns of $x \in \mathbb{R}^{m\times m}$, $\|x\|_1 = \sum_{i=1}^{m^2}|x_i|$ and $\|x\|_2 = \sqrt{\sum_{i=1}^{m^2}|x_i|^2}$. That is, we find the decrypted (hidden) image $x^* \in \mathbb{R}^{m\times m}$ that solves

$$\min_{x\in\mathbb{R}^{m\times m}}\left\{\left\|Ax - L^\dagger\right\|_2^2 + \kappa_1\|x\|_1\right\} \tag{4.3}$$

and such that the watermark (superposition images) extracted image $y^* = Ax^* \in \mathbb{R}^{m\times m}$ solves

$$\min_{y=Ax\in\mathbb{R}^{m\times m}}\left\{\left\|\rho(Ax) - \left(M - \sum_{i=1}^{N}\beta_i C_i\right)\right\|_2^2 + \kappa_2\|Ax\|_1\right\}. \tag{4.4}$$

It is well known from Lemma 2.2 by putting $T(Ax) = P_{\mathbb{R}^{m\times m}}Ax = L^\dagger$ that $\nabla F_1(x) = 2A^T(Ax - L^\dagger)$ and ∇F_1 is $\frac{1}{\psi_1}$-Lipschitzian such that $\psi_1 = \frac{1}{2\|A\|^2}$, and putting $T(\rho(Ax)) = P_{\mathbb{R}^{m\times m}}\rho(Ax) = M - \sum_{i=1}^{N}\beta_i C_i$ that $\nabla F_2(x) = 2\rho A^T(\rho(Ax) - (M - \sum_{i=1}^{N}\beta_i C_i))$ and ∇F_2 is $\frac{1}{\psi_2}$-Lipschitzian such that $\psi_2 = \frac{1}{2\rho^2\|A\|^2}$, and A^T stands for the transpose of A, and $\|A\|$ is the largest singular

value of A (i.e., the square root of the largest eigenvalue of the matrix A^TA) or the spectral norm $\|A\|_2$.

By [29] and the references therein, for $(u_1, u_2, \ldots, u_{m^2})^T, (\tilde{u}_1, \tilde{u}_2, \ldots, \tilde{u}_{m^2})^T \in \mathbb{R}^{m^2}$ corresponding with stacking the columns of $u, \tilde{u} \in \mathbb{R}^{m\times m}$, respectively, and for each $n \in \mathbb{N}$, we have

$$\operatorname{prox}_{\lambda_n G_1}(u) = \operatorname{prox}_{\lambda_n \kappa_1 \|u\|_1}(u) = v \quad \text{and} \quad \operatorname{prox}_{\eta_n G_2}(\tilde{u}) = \operatorname{prox}_{\eta_n \kappa_2 \|A\tilde{u}\|_1}(\tilde{u}) = \tilde{v},$$

where $v_i = \operatorname{sign}(u_i)\max\{|u_i| - \lambda_n\kappa_1, 0\}$ and $\tilde{v}_i = \operatorname{sign}(\tilde{u}_i)\max\{|(A\tilde{u})_i| - \eta_n\kappa_2, 0\}$ for all $i = 1, 2, \ldots, m^2$ such that $(v_1, v_2, \ldots, v_{m^2})^T, (\tilde{v}_1, \tilde{v}_2, \ldots, \tilde{v}_{m^2})^T \in \mathbb{R}^{m^2}$ corresponding to stacking the columns of $v, \tilde{v} \in \mathbb{R}^{m\times m}$, respectively.

Example 4.2 We illustrate the performance of FBSA_Err in Algorithm 1 for solving image-feature extraction with the multiple-image blends problem through (4.3) and (4.4) with $\kappa_1 = \kappa_2 = 10^{-4}$. We implemented them in MATLAB R2019a to solve and run on a personal laptop: Intel(R) Core(TM) i5-8250U CPU @1.80 GHz 8 GB RAM.

Let $x = (a_{ij})$, $x_n = (b_{ij}) \in \mathbb{R}^{m\times m}$ represent the hidden image and the estimated image at the first n iteration(s), respectively. We use the normalized crosscorrelation (NCC) as the digital image-matching measure (it is better if this is near 1) of the images x and x_n, which is defined by

$$\operatorname{NCC}(x, x_n) = \frac{\sum_{i=1}^m \sum_{j=1}^m [(a_{ij} - \bar{a})(b_{ij} - \bar{b})]}{\sqrt{[\sum_{i=1}^m \sum_{j=1}^m (a_{ij} - \bar{a})^2][\sum_{i=1}^m \sum_{j=1}^m (b_{ij} - \bar{b})^2]}},$$

where $\bar{a} = \frac{1}{m^2}\sum_{i=1}^m \sum_{j=1}^m a_{ij}$ and $\bar{b} = \frac{1}{m^2}\sum_{i=1}^m \sum_{j=1}^m b_{ij}$, and also use the signal-to-noise ratio (SNR) measure (it is better if this is a large value) of the images x and x_n, and the improvement in signal-to-noise ratio (ISNR) measure (it is better if this is a large value) of the

Algorithm 1 The image-feature extraction with multiple-image blends algorithm

procedure FBSA_Err1

Choose the initials $x_0, x_1 \in \mathbb{R}^{m\times m}$ arbitrarily.

Set M as the maximum loops to stop.

Set the operator A and the mapping f in backing tracks.

$n \leftarrow 0$

repeat

$n \leftarrow n + 1$

Update the parameters α_n, γ_n, λ_n, η_n, θ_n and the errors $\varepsilon_n, \xi_n \in \mathbb{R}^{m\times m}$.

% Hadamard product (element-wise multiplication) is used in the processes.

$z_n \leftarrow x_n + \theta_n(x_n - x_{n-1})$

$y_n \leftarrow z_n + \gamma_n A^T(\operatorname{prox}_{\eta_n G_2}(Az_n - 2\rho\eta_n A^T(\rho(A^2 z_n) - (M - \sum_{i=1}^N \beta_i C_i)) + \xi_n) - Az_n)$

$x_{n+1} \leftarrow \alpha_n f(y_n) + (1 - \alpha_n)\operatorname{prox}_{\lambda_n G_1}(y_n - 2\lambda_n A^T(Ay_n - L^\dagger) + \varepsilon_n)$

until $n = M$

return x_{n+1}

end procedure

images x, x_n and $L^\dagger$, which are defined (measured in decibels: dB) by

$$\mathrm{SNR}(x, x_n) = 10\log_{10}\frac{\|x_n\|_2^2}{\|x - x_n\|_2^2} \quad \text{and}$$

$$\mathrm{ISNR}\left(x, x_n, L^\dagger\right) = 10\log_{10}\frac{\|x - L^\dagger\|_2^2}{\|x - x_n\|_2^2},$$

where $L^\dagger \in \mathbb{R}^{m\times m}$ represents the observed encrypted image with additive noise.

For illustration, we consider the standard test images downloaded from [41] for Woman, Pirate, and Cameraman, and image information downloaded from [42] with all images converted to the double class type of a monochrome image and resized to 256×256 pixels by img = im2double(imread('image_name')) and imresize(img,[256,256]) in MATLAB, respectively, which represent the carrier images $C_1, C_2, C_3 \in \mathbb{R}^{256\times256}$ and the hidden image $H \in \mathbb{R}^{256\times256}$, respectively, see Fig. 2.

The hidden image H went through chaos-based image encryption, to an encrypted image $L = A * H$ such that stacking the columns of $A \in \mathbb{R}^{256\times256}$ corresponding with discrete logistic chaotic map $\tilde{x} = \{x_n\}_{n=1}^{256^2}$ with $\mu = 3.57$ and the logistic chaotic map initial $x_1 = 0.25$ by $A = \mathrm{reshape}(\tilde{x}, [256, 256])$ and $L = A. * H$ in MATLAB, and followed by adding the zero-mean white Gaussian noise ε with standard deviation 10^{-3} to the image $L^\dagger = L + \varepsilon = L + 10^{-3} * \mathrm{randn}(\mathrm{size}(L))$ in MATLAB, see Fig. 3.

The encrypted image with additive noise $L^\dagger$ went through image mixing of superposition carrier images of C_1 = Woman, C_2 = Pirate, and C_3 = Cameraman, respectively, to the superimposed mixed image M with $\mu_1 = 0.999$, $\mu_2 = 0.25$, and $\mu_3 = 0.5$ as fol-

Figure 2 Hidden image and carrier images

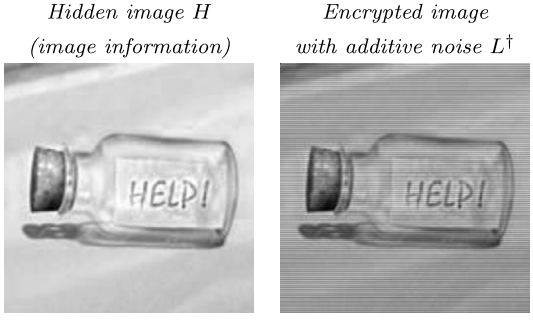

Figure 3 Hidden image and encrypted image with additive noise

lows:

$$M_1 = \mu_1 C_1 + (1 - \mu_1)L^\dagger,$$
$$M_2 = \mu_2 C_2 + (1 - \mu_2)M_1,$$
$$M_3 = \mu_3 C_3 + (1 - \mu_3)M_2,$$

or

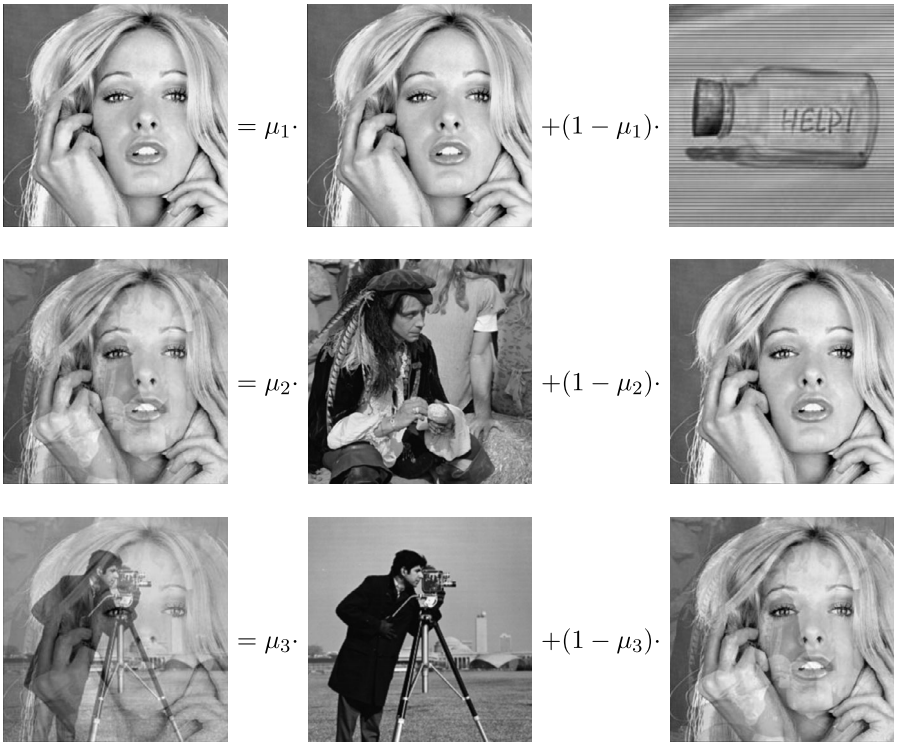

where $M = M_3$. That is,

$$M = \rho L^\dagger + \beta_1 C_1 + \beta_2 C_2 + \beta_3 C_3$$

such that $\rho = (1 - \mu_1)(1 - \mu_2)(1 - \mu_3) = 0.000375$, $\beta_1 = (1 - \mu_2)(1 - \mu_3)\mu_1 = 0.3746$, $\beta_2 = (1 - \mu_3)\mu_2 = 0.125$ and $\beta_3 = \mu_3 = 0.5$, and $L^\dagger$, M_1, M_2, and M_3 are as in Fig. 4. We now find the decrypted (hidden) image $x^* \in \mathbb{R}^{256\times256}$ that solves

$$\min_{x\in\mathbb{R}^{256\times256}} \left\{ \left\| Ax - L^\dagger \right\|_2^2 + \kappa_1 \|x\|_1 \right\}$$

and such that the watermark (superposition images) extracted image $y^* = Ax^* \in \mathbb{R}^{256\times256}$ solves

$$\min_{y=Ax\in\mathbb{R}^{256\times256}} \left\{ \left\| \rho(Ax) - \left(M - \sum_{i=1}^{3} \beta_i C_i \right) \right\|_2^2 + \kappa_2 \|Ax\|_1 \right\}.$$

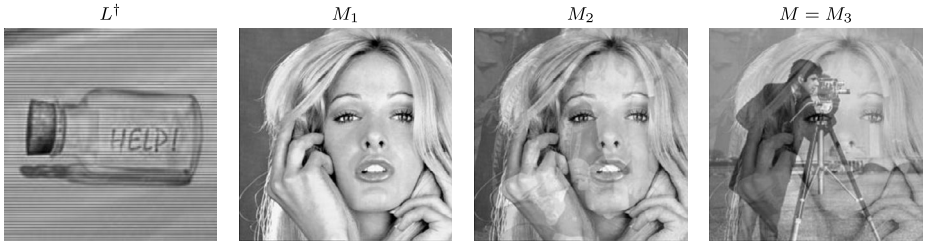

Figure 4 Encrypted image with additive noise $L^\dagger$ and superimposed mixed images M_1, M_2, and M_3

Table 1 The best choice types of testing the parameters γ_n, λ_n, and η_n for the fast convergence

Type	γ_n	λ_n	η_n
A1	$\frac{L_0}{10}$	$\frac{L_1}{10}$	$\frac{L_2}{10}$
A2	$L_0 - \frac{L_0}{10}$	$L_1 - \frac{L_1}{10}$	$L_2 - \frac{L_2}{10}$
A3	L_0	L_1	L_2
A4	$L_0 + \frac{L_0}{10}$	$L_1 + \frac{L_1}{10}$	$L_2 + \frac{L_2}{10}$
A5	$2L_0 - \frac{L_0}{10}$	$2L_1 - \frac{L_1}{10}$	$2L_2 - \frac{L_2}{10}$
A6	–	$2L_1$	$2L_2$
B1	$\frac{L_0 n}{n+1}$	$\frac{L_1 n}{n+1}$	$\frac{L_2 n}{n+1}$
B2	$\frac{L_0(n+2)}{n+1}$	$\frac{L_1(n+2)}{n+1}$	$\frac{L_2(n+2)}{n+1}$
B3	–	$\frac{2L_1 n}{n+1}$	$\frac{2L_2 n}{n+1}$
C1	$L_0 + \frac{(-1)^n L_0}{n+1}$	$L_1 + \frac{(-1)^n L_1}{n+1}$	$L_2 + \frac{(-1)^n L_2}{n+1}$
C2	$L_0 + \frac{(-1)^{n+1} L_0}{n+1}$	$L_1 + \frac{(-1)^{n+1} L_1}{n+1}$	$L_2 + \frac{(-1)^{n+1} L_2}{n+1}$

Let $L = \|A\|^2$, $\psi_1 = \frac{1}{2\|A\|^2} = \frac{1}{2L}$ and $\psi_2 = \frac{1}{2\rho^2\|A\|^2} = \frac{1}{2\rho^2 L}$. We introduce the best choice types of testing the parameters γ_n, λ_n and η_n for the fast convergence with $L_0 = \frac{1}{2L}$, $L_1 = \psi_1$, and $L_2 = \psi_2$ as in Table 1. For each $n \in \mathbb{N}$, we assume the parameters λ_n and η_n are A6 type, which is the best choice type for all cases of the parameter γ_n, and setting $\alpha_n = \frac{10^{-6}}{n+1}$ and

$$\theta_n = \begin{cases} \sigma_n = \frac{t_n - 1}{t_{n+1}} \quad \text{such that } t_1 = 1 \text{ and } t_{n+1} = \frac{1+\sqrt{1+4t_n^2}}{2} & \text{if } n \le 1000, \\ \begin{cases} \min\{\frac{1/(n+1)^3}{\|x_n - x_{n-1}\|}, \alpha_n\} & \text{if } x_n \ne x_{n-1}, \\ \alpha_n & \text{otherwise,} \end{cases} & \text{otherwise,} \end{cases} \tag{4.5}$$

and the errors $\varepsilon_n = \xi_n = \frac{M}{(n+1)^3}$, and we also set $f(x) = \frac{x}{5}$ for all $x \in \mathbb{R}^{256\times 256}$ and choose the algorithm initials $x_0 = x_1 = M$.

We use NCC, SNR, and ISNR that measure the quality of the decrypted image at the first 10,000 iterations, which are shown in Table 2. Moreover, we also show the relative error that is defined by

$$\frac{\|x_{n+1} - x_n\|_2}{\|x_n\|_2} \le \text{tol},$$

where tol denotes a prescribed tolerance value of the algorithm, and their convergence behaviors are shown in Fig. 5.

Table 2 All cases of the parameter γ_n (with A6 type of the parameters λ_n and η_n) at the first 10,000 iterations

Case	γ_n	λ_n	η_n	CPU (s)	NCC	SNR	ISNR	tol
1	A1	A6	A6	425.51	0.9924	19.4825	9.8366	2.42×10^{-7}
2	A2	A6	A6	429.86	0.9763	23.5064	14.4992	2.52×10^{-7}
3	A3	A6	A6	431.31	0.9687	23.4392	14.5077	2.57×10^{-7}
4	A4	A6	A6	425.90	0.9572	23.1888	14.3321	2.65×10^{-7}
5	A5	A6	A6	425.94	0.7978	18.5734	10.2851	3.59×10^{-7}
6	B1	A6	A6	434.32	0.9689	23.4424	14.5101	2.57×10^{-7}
7	B2	A6	A6	430.61	0.9686	23.4359	14.5052	2.58×10^{-7}
8	C1	A6	A6	430.83	0.9687	23.4392	14.5077	2.57×10^{-7}
9	C2	A6	A6	440.86	0.9687	23.4392	14.5077	2.57×10^{-7}

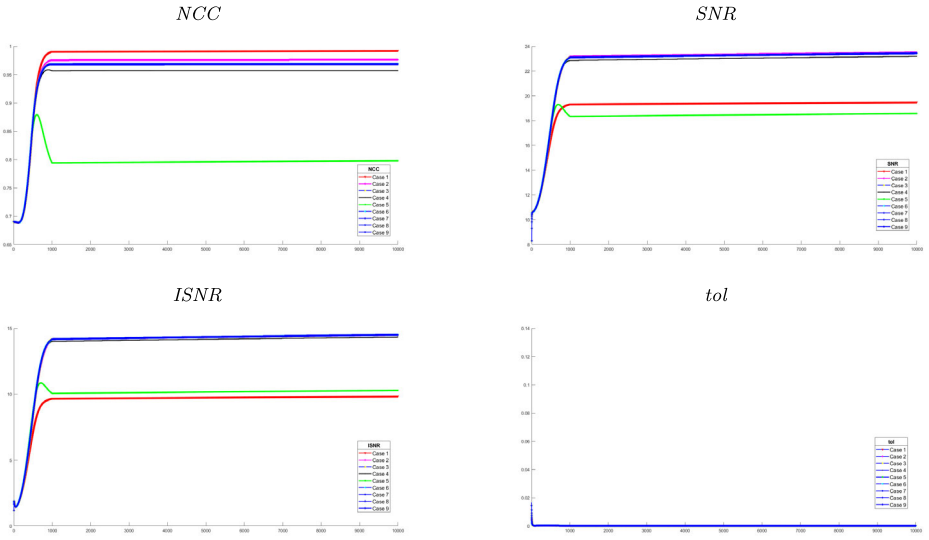

Figure 5 Convergence behaviors of NCC, SNR, ISNR and tol

From the results of all quality measures of the feature-extracted image as in Table 2, we see that the quantity of NCC in cases 1 and 2 are greater than the others, but the quantities of SNR and ISNR of them are lower and greater than others, respectively, and then, we conclude that for quality measure of the decrypted image by NCC measure only, case 1 is the best choice, and by NCC, SNR, and ISNR measures together, case 2 is the best choice, for image-feature extraction with multiple-image blends using FBSA_Err, which are shown in Figs. 6, 7, and 8, and also show the increasing of NCC, SNR, and ISNR of them in the first 10,000 to 100,000 iterations as in Table 3.

We next consider seven different choices of the parameter θ_n for testing the fast convergence at the first 10,000 iterations of the case 2 only, as follows: $\sigma_n = \frac{1}{2^n}$ (choice 1), $\sigma_n = \frac{1}{n+1}$ (choice 2), $\sigma_n = 0$ (choice 3), $\sigma_n = 0.5$ (choice 4), $\sigma_n = \frac{n}{n+1}$ (choice 5), $\sigma_n = \frac{t_n - 1}{t_{n+1}}$ such that $t_1 = 1$ and $t_{n+1} = \frac{1+\sqrt{1+4t_n^2}}{2}$ (choice 6) of

$$\theta_n = \begin{cases} \sigma_n & \text{if } n \leq 1000, \\ \begin{cases} \min\{\frac{1/(n+1)^3}{\|x_n - x_{n-1}\|}, \alpha_n\} & \text{if } x_n \neq x_{n-1}, \\ \alpha_n & \text{otherwise,} \end{cases} & \text{otherwise} \end{cases} \tag{4.6}$$

Figure 6 The best feature extracted images of cases 1 and 2

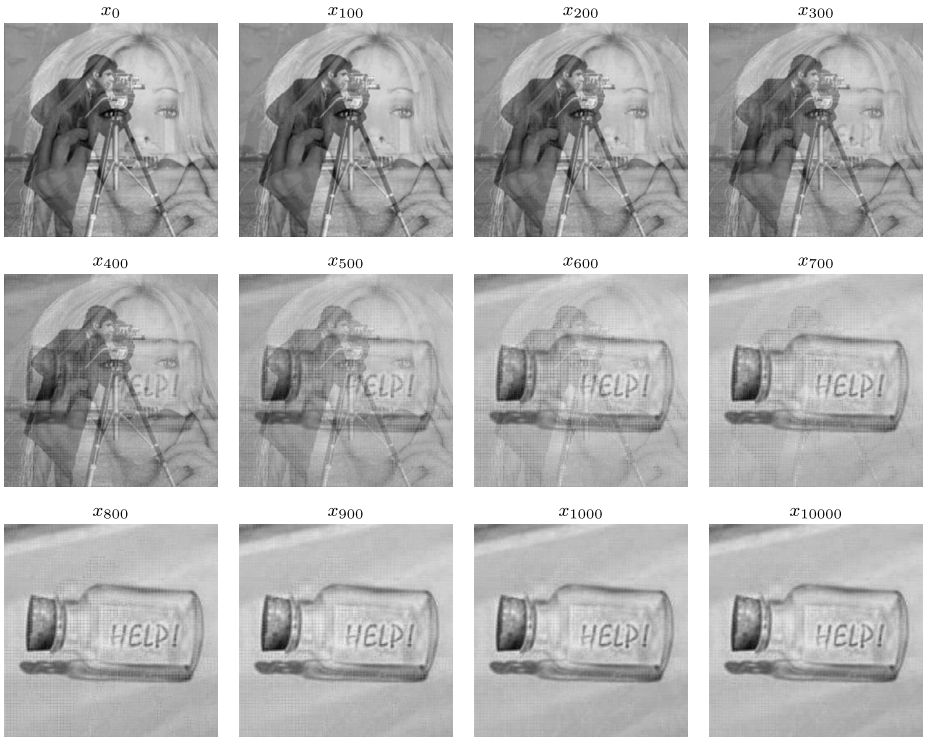

Figure 7 Convergence behavior of the image x_n in case 1

and choice 7 is

$$\theta_n = \begin{cases} \min\{\frac{1/(n+1)^3}{\|x_n - x_{n-1}\|}, 0.5\} & \text{if } x_n \neq x_{n-1}, \\ 0.5 & \text{otherwise,} \end{cases} \tag{4.7}$$

and the others constant.

From the results of seven different choices of the parameter θ_n as in Table 4, we see that all quality measures of choice 6 are greater than the others, and then we conclude that the choice 6 of the parameter θ_n as (4.5) is to be an accelerated choice for the speed up of convergence of solving this complex example.

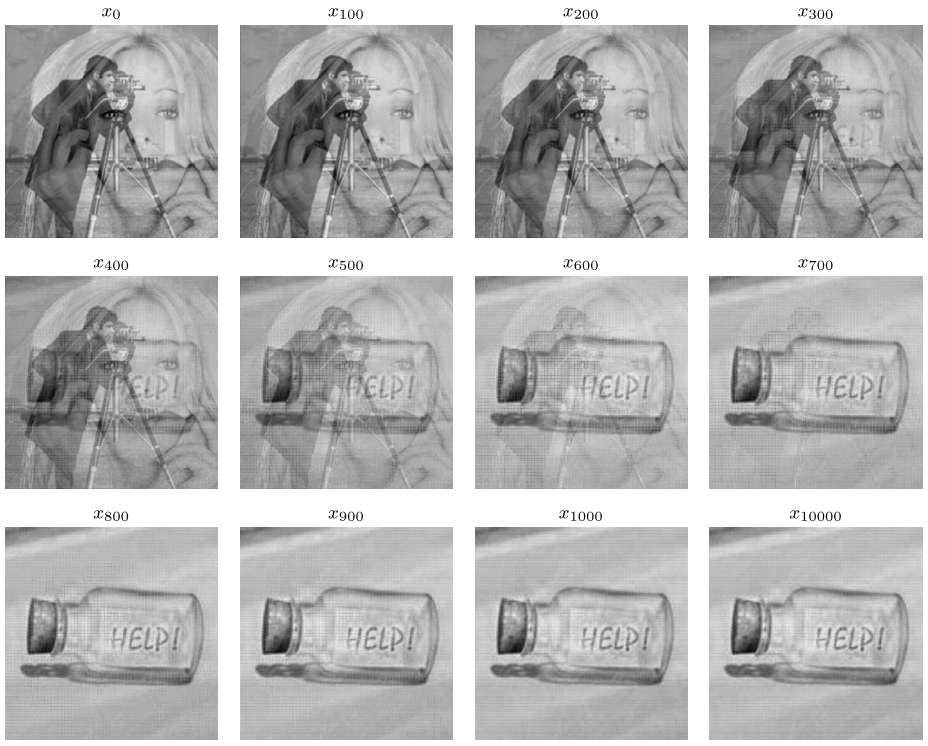

Figure 8 Convergence behavior of the image x_n in case 2

Table 3 The increasing of NCC, SNR, and ISNR of cases 1 and 2

Case 1				Case 2			
n	NCC	SNR	ISNR	*n*	NCC	SNR	ISNR
10,000	0.9924	19.4825	9.8366	10,000	0.9763	23.5064	14.4992
25,000	0.9941	19.6572	10.0205	25,000	0.9768	23.8564	14.8513
50,000	0.9954	19.8115	10.1833	50,000	0.9769	24.1426	15.1397
75,000	0.9961	19.8835	10.2593	75,000	0.9769	24.2643	15.2628
100,000	0.9964	19.9184	10.2960	100,000	0.9769	24.3201	15.3195

Table 4 Choices of the parameter θ_n for testing fast convergence at the first 10,000 iterations

Choice	CPU (s)	NCC	SNR	ISNR	tol
1	469.60	0.7163	12.5216	4.3232	5.49×10^{-6}
2	470.78	0.7151	12.7150	4.3570	5.14×10^{-6}
3	470.51	0.7180	12.1811	4.1980	6.03×10^{-6}
4	463.59	0.7158	13.1323	4.1536	4.09×10^{-6}
5	471.47	0.5356	6.4557	−1.3499	9.50×10^{-6}
6	429.86	0.9763	23.5064	14.4992	2.52×10^{-7}
7	468.06	0.7180	12.1859	4.2001	6.02×10^{-6}

Remark 4.3 The architecture of the chaos-based image cryptosystem mainly consists of two stages: the confusion (pixel permutation) stage and the diffusion (sequential pixel-value modification) stage, which are directly generated by the point-spread function A on pixels of the hidden image H to the encrypted image $L = A \diamond H$ (pixel permutation or sequential pixel-value modification of H by A). In this paper, the hidden image H encrypts of the confusion stage to the encrypted image $L = A * H$, which is generated by the linear

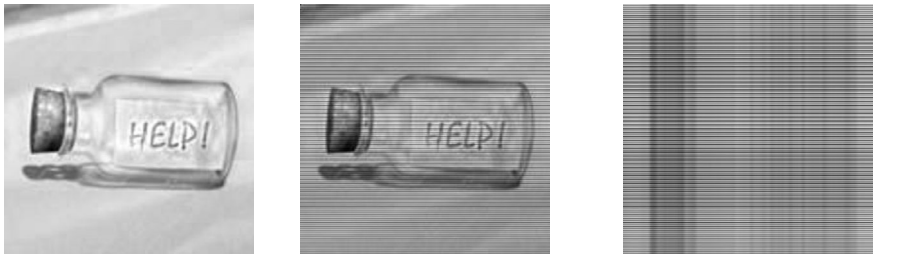

Figure 9 Encrypted images using linear method

method of element-wise multiplication of A and H such that stacking the columns of $A \in \mathbb{R}^{m\times m}$ corresponding with the discrete logistic chaotic map $\{x_n\}_{n=1}^{m^2}$. For the diffusion stage using this linear method, the encrypted image L can be generated by $L = A \cdot H$ (regular matrix multiplication of A and H) as in Fig. 9.

Open problem How to write a programming technique of FBSA_Err to solve the image-feature extraction with multiple-image blends problem of the encrypted image $L = A \cdot H$?

4.2 Split minimization problem

Let $G_1 : H_1 \to \mathbb{R} \cup \{\infty\}$ and $G_2 : H_2 \to \mathbb{R} \cup \{\infty\}$ be two convex and lower semicontinuous functions. If $f_1 = f_2 = 0$ and $B_1 = \partial G_1$, and $B_2 = \partial G_2$ then the SMVIP is reduced to the split variational inclusion problem (SVIP) or the split minimization problem (SMP), which is to find $x^* \in H_1$ such that

$$G_1(x^*) = \min_{x\in H_1} G_1(x) \quad \Leftrightarrow \quad 0 \in \partial G_1(x^*) \tag{4.8}$$

and such that $y^* = Ax^* \in H_2$ solves

$$G_2(y^*) = \min_{y=Ax\in H_2} G_2(y) \quad \Leftrightarrow \quad 0 \in \partial G_2(y^*) \tag{4.9}$$

and we will denote by Φ the solution set of (4.8) and (4.9). That is,

$$\Phi = \{x \in H_1 : x \text{ solves (4.8) and } y = Ax \text{ solves (4.9)}\}.$$

Many researchers have proposed, analyzed, and modified the iteration methods for solving the SMVIP and the SVIP using self-adaptive, step-size methods. Recently, Yao et al. [43] introduced the YSLD method in Algorithm 2.1 for solving SMVIP, and also Tan et al. [44] introduced TQY methods in Algorithms 3.3 and 3.4, and Thong et al. [45] introduced the TDC method in Algorithm 3.3 for solving SVIP, as follows.

Let H_1, H_2, A, f_1, f_2, B_1, B_2, and f be defined as the state of Theorem 3.1, and assume that Ω and Φ are nonempty and satisfy the condition (A).

YSLD method in Algorithm 2.1 Let $x_0, x_1 \in H_1$ and $\{x_n\} \subset H_1$ be a sequence generated by

$$\begin{cases} z_n = x_n + \theta_n(x_n - x_{n-1}), \\ y_n = z_n + \gamma_n A^*(J_\lambda^{B_2}(I - \lambda f_2)Az_n) - Az_n), \\ x_{n+1} = J_\lambda^{B_1}(I - \lambda f_1)y_n, \end{cases}$$

for all $n \in \mathbb{N}$, where $\theta_n \in [0, \bar{\theta_n}]$, $\lambda \in (0, 2\psi)$ such that $\psi = \min\{\psi_1, \psi_2\}$ and

$$\bar{\theta_n} = \begin{cases} \min\{\frac{\omega_n}{\|x_n - x_{n-1}\|^2}, \theta\}, & x_n \neq x_{n-1}, \\ \theta, & \text{otherwise}, \end{cases}$$

and

$$\gamma_n = \begin{cases} \frac{\rho_n \|J_\lambda^{B_2}(I-\lambda f_2)Az_n - Az_n\|^2}{\|A^*(J_\lambda^{B_2}(I-\lambda f_2)Az_n - Az_n)\|^2}, & J_\lambda^{B_2}(I - \lambda f_2)Az_n - Az_n \neq 0, \\ \gamma, & \text{otherwise}, \end{cases}$$

such that $\rho_n \in [a, b] \subset (0, 1)$, $\{\omega_n\} \in \ell_1$, $\theta \in [0, 1)$ and $\gamma > 0$.

TQY method in Algorithm 3.3 Let $x_0, x_1 \in H_1$ and $\{x_n\} \subset H_1$ be a sequence generated by

$$\begin{cases} z_n = x_n + \theta_n(x_n - x_{n-1}), \\ y_n = J_\lambda^{B_1}(z_n - \gamma_n A^*(I - J_\lambda^{B_2})Az_n), \\ x_{n+1} = (1 - \alpha_n - \beta_n)z_n + \beta_n y_n, \end{cases}$$

for all $n \in \mathbb{N}$, where $\{\alpha_n\}, \{\beta_n\} \subset (0, 1)$ such that $\lim_{n\to\infty} \alpha_n = 0$, $\sum_{n=1}^{\infty} \alpha_n = \infty$, $\{\beta_n\} \subset (a, b) \subset (0, 1 - \alpha_n)$, and

$$\theta_n = \begin{cases} \min\{\frac{\omega_n}{\|x_n - x_{n-1}\|}, \theta\}, & x_n \neq x_{n-1}, \\ \theta, & \text{otherwise}, \end{cases} \tag{4.10}$$

and

$$\gamma_n = \begin{cases} \frac{\rho_n \|(I-J_\lambda^{B_2})Az_n\|^2}{\|A^*(I-J_\lambda^{B_2})Az_n\|^2}, & \|A^*(I - J_\lambda^{B_2})Az_n\| \neq 0, \\ \gamma, & \text{otherwise}, \end{cases} \tag{4.11}$$

such that $\theta > 0$, $\gamma > 0$, $\lambda > 0$, $\rho_n \in (0, 2)$, $\omega_n = o(\alpha_n)$ and $\lim_{n\to\infty} \frac{\omega_n}{\alpha_n} = 0$.

TQY method in Algorithm 3.4 Let $x_0, x_1 \in H_1$ and $\{x_n\} \subset H_1$ be a sequence generated by

$$\begin{cases} z_n = x_n + \theta_n(x_n - x_{n-1}), \\ y_n = J_\lambda^{B_1}(z_n - \gamma_n A^*(I - J_\lambda^{B_2})Az_n), \\ x_{n+1} = \alpha_n f(x_n) + (1 - \alpha_n)y_n, \end{cases}$$

for all $n \in \mathbb{N}$, where $\{\alpha_n\} \subset (0,1)$ such that $\lim_{n\to\infty} \alpha_n = 0$, $\sum_{n=1}^{\infty} \alpha_n = \infty$, θ_n defined as (4.10) and γ_n defined as (4.11) such that $\theta > 0$, $\gamma > 0$, $\lambda > 0$, $\rho_n \in (0,2)$, $\omega_n = o(\alpha_n)$ and $\lim_{n\to\infty} \frac{\omega_n}{\alpha_n} = 0$.

TDC method in Algorithm 3.3 Let $x_0, x_1 \in H_1$ and $\{x_n\} \subset H_1$ be a sequence generated by

$$\begin{cases} z_n = x_n + \theta_n(x_n - x_{n-1}), \\ y_n = J_\lambda^{B_1}(z_n - \gamma_n A^*(I - J_\lambda^{B_2})Az_n), \\ x_{n+1} = (1-\alpha_n)(z_n - \beta_n d(z_n, y_n)) + \alpha_n f(x_n), \end{cases}$$

for all $n \in \mathbb{N}$, where $\theta_n \in [0, \bar{\theta_n}]$, $\{\alpha_n\} \subset (0,1)$, $\{\gamma_n\} \subset [a,b] \subset (0, \frac{1}{L})$ such that $L = \|A\|^2$, $\lim_{n\to\infty} \alpha_n = 0$, $\sum_{n=1}^{\infty} \alpha_n = \infty$ and

$$\bar{\theta_n} = \begin{cases} \min\{\frac{\omega_n}{\|x_n - x_{n-1}\|}, \theta\}, & x_n \neq x_{n-1}, \\ \theta, & \text{otherwise}, \end{cases}$$

and

$$\beta_n = \frac{\langle z_n - y_n, d(z_n, y_n)\rangle}{\|d(z_n, y_n)\|^2}$$

such that

$$d(z_n, y_n) = z_n - y_n - \gamma_n\big(A^*\big(I - J_\lambda^{B_2}\big)Az_n - A^*\big(I - J_\lambda^{B_2}\big)Ay_n\big)$$

and $\theta > 0$, $\lambda > 0$, $\omega_n = o(\alpha_n) \in [0, \theta)$, and $\lim_{n\to\infty} \frac{\omega_n}{\alpha_n} = 0$.

Example 4.4 We illustrate the performance of our Algorithm 2 in Theorem 3.1 compared with the YSLD Algorithm 2.1, TQY Algorithms 3.3 and 3.4, and the TDC Algorithm 3.3. We implemented them in MATHEMATICA 5.0 to solve and run on a personal laptop: Intel(R) Core(TM) i5-8250U CPU @1.80 GHz 8 GB RAM.

Let $H_1 = H_2 = L^2([0,1])$ embedded with the inner product $\langle x(t), y(t)\rangle = \int_0^1 x(t)y(t)\,dt$ and the induced norm $\|x(t)\| = (\int_0^1 |x(t)|^2\,dt)^{1/2}$ for all $x(t), y(t) \in L^2([0,1])$. Let $A : L^2([0,1]) \to L^2([0,1])$ be the Volterra integration operator, which is given by $(Ax)(t) = \int_0^t x(s)\,ds$ for all $t \in [0,1]$ and $x(t) \in L^2([0,1])$. It is well known that the adjoint A^* of A, which is defined by $(A^*x)(t) = \int_t^1 x(s)\,ds$ for all $t \in [0,1]$ and $x(t) \in L^2([0,1])$, is a bounded linear operator and $\|A\| = \frac{2}{\pi}$ (see [46]).

Let $f_1 = f_2 = 0$ and $B_1 = \partial\|x(t)\|$, $B_2 = \partial\|y(t)\|$ with $y(t) = Ax$ for all $x(t), y(t) \in L^2([0,1])$. Then, the SMVIP and the SVIP are reduced to finding $x^*(t) \in L^2([0,1])$ such that

$$\big\|x^*(t)\big\| = \min_{x(t)\in L^2([0,1])} \big\|x(t)\big\| \quad \Leftrightarrow \quad 0 \in \partial\big\|x^*(t)\big\|$$

and such that $y^*(t) = Ax^* \in L^2([0,1])$ solves

$$\big\|y^*(t)\big\| = \min_{y(t)=Ax\in L^2([0,1])} \big\|y(t)\big\| \quad \Leftrightarrow \quad 0 \in \partial\big\|y^*(t)\big\|.$$

Algorithm 2 The forward–backward splitting algorithm with errors

procedure FBSA_Err2

Choose the initials $x_0, x_1 \in H_1$ arbitrarily. Set the error ϵ.

Set the operator A, and the mapping f in backing tracks.

$n \leftarrow 0$

repeat

$n \leftarrow n+1$

Update the parameters α_n, γ_n, λ_n, η_n, θ_n and the errors $\varepsilon_n \in H_1$ and $\xi_n \in H_2$.

$z_n \leftarrow x_n + \theta_n(x_n - x_{n-1})$

$y_n \leftarrow z_n + \gamma_n A^*(J^{B_2}_{\eta_n}((I-\eta_n f_2)Az_n + \xi_n) - Az_n)$

$x_{n+1} \leftarrow \alpha_n f(y_n) + (1-\alpha_n)J^{B_1}_{\lambda_n}((I-\lambda_n f_1)y_n + \varepsilon_n)$

until $\|x_{n+1} - x_n\| < \epsilon$

return x_{n+1}

end procedure

Table 5 Numerical results of Example 4.4 for $\psi_1 = \psi_2 = 1$

Algorithms	$x_0 = x_1 = 15$		$x_0 = x_1 = 20t^2 + t$		$x_0 = x_1 = 20\sin(t)$		$x_0 = x_1 = 5e^t$	
($\psi_1 = \psi_2 = 1$)	n	CPU (s)	n	CPU (s)	n	CPU (s)	n	CPU (s)
Our Alg. 2	5	0.6880	5	1.1710	5	2.3760	4	0.7660
YLSD Alg. 2.1	6	0.9220	6	1.6250	6	2.0940	5	2.1410
TQY Alg. 3.3	7	3.9380	6	2.9060	7	4.9690	6	3.1710
TQY Alg. 3.4	7	2.1090	6	2.5470	6	2.2500	5	2.1710

Note that $(x(t), y(t)) = (0,0) \in \Omega = \Phi$. For $\lambda > 0$ and $x(t) \in L^2([0,1])$, by [43] we have

$$\left(J^{B_1}_{\lambda}x\right)(t) = \begin{cases} x - \frac{\lambda x}{\|x\|}, & \|x\| > \lambda, \\ 0, & \|x\| \le \lambda, \end{cases} \quad \text{and} \quad \left(J^{B_2}_{\lambda}x\right)(t) = \begin{cases} x - \frac{\lambda Ax}{\|Ax\|}, & \|Ax\| > \lambda, \\ x - Ax, & \|Ax\| \le \lambda. \end{cases}$$

In the compared algorithms, all parameters have been set to their high performance. Since, f_1 and f_2 are ψ_1 and ψ_2 inverse strongly monotones for all $\psi_1, \psi_2 > 0$, respectively, we fix $\psi_1 = \psi_2$ and let $L = \|A\|^2$, $L_0 = \frac{1}{2L}$, $L_1 = \psi_1$ and $L_2 = \psi_2$.

For each $n \in \mathbb{N}$, we set $\alpha_n = \frac{10^{-10}}{n+1}$, $\beta_n = (1-10^{-10})(1-\alpha_n)$, $\gamma_n = L_0$ (A3 type in Table 2 for our Alg. 2 and TDC Alg. 3.3), $\lambda_n = 2L_1$ (A6 type in Table 2), $\lambda = 2L_1 - 0.01$ (for YLSD Alg. 2.1), $\lambda = 2L_1$ (for TQY Algs. 3.3 and 3.4, and TDC Alg. 3.3), $\eta_n = 2L_2$ (A6 type in Table 2), θ_n (for our Alg. 2) is as (4.5), $\theta_n = \bar{\theta_n}$ (for YSLD Alg. 2.1 and TDC Alg. 3.3), $\omega_n = \frac{1}{(n+1)^2}$, $\rho_n = \theta = \gamma = 0.5$, the errors $\varepsilon_n(t) = \xi_n(t) = \frac{1}{(n+1)^3}$ and $f(x(t)) = \frac{x}{5}$ for all $x(t) \in L^2([0,1])$.

We use $\|x_{n+1} - x_n\| < \epsilon$ such that the error $\epsilon = 10^{-10}$ is the stopping criterion in the process of all compared algorithms. The numerical results are shown in Table 5 (for $\psi_1 = \psi_2 = 1$), Table 6 (for $\psi_1 = \psi_2 = 10$), and Table 7 (for $\psi_1 = \psi_2 = 20$), and the convergence behaviors of the error sequences $\{\|x_{n+1} - x_n\|\}$ are shown in Fig. 10 (for $\psi_1 = \psi_2 = 1$ only) with four different initial functions $x_0(t) = x_1(t)$ (except for the TDC Algorithm 3.3 because their convergence is slow). Moreover, we also show the approximate solution functions of some case studies via the speed up of convergence from increased values $\psi_1 = \psi_2 = 1, 10, 20$ with initial functions $x_0(t) = x_1(t) = 15$, see Fig. 11.

Table 6 Numerical results of Example 4.4 for $\psi_1 = \psi_2 = 10$

Algorithms	$x_0 = x_1 = 15$		$x_0 = x_1 = 20t^2 + t$		$x_0 = x_1 = 20\sin(t)$		$x_0 = x_1 = 5e^t$	
($\psi_1 = \psi_2 = 10$)	n	CPU (s)	n	CPU (s)	n	CPU (s)	n	CPU (s)
Our Alg. 2	3	0.2030	3	4.2960	3	0.6100	2	0.2030
YLSD Alg. 2.1	2	0.0620	2	0.1100	2	0.1870	2	0.2190
TQY Alg. 3.3	3	0.0620	3	0.1870	3	0.2970	3	0.2960
TQY Alg. 3.4	3	0.0780	2	0.1100	3	0.3270	2	0.2340

Table 7 Numerical results of Example 4.4 for $\psi_1 = \psi_2 = 20$

Algorithms	$x_0 = x_1 = 15$		$x_0 = x_1 = 20t^2 + t$		$x_0 = x_1 = 20\sin(t)$		$x_0 = x_1 = 5e^t$	
($\psi_1 = \psi_2 = 20$)	n	CPU (s)	n	CPU (s)	n	CPU (s)	n	CPU (s)
Our Alg. 2	3	0.1870	3	4.2970	3	0.5780	2	0.2030
YLSD Alg. 2.1	2	0.0620	2	0.1560	2	0.2190	2	0.2500
TQY Alg. 3.3	3	0.0780	3	0.2030	3	0.2810	3	0.2810
TQY Alg. 3.4	3	0.0780	2	0.1100	3	0.2810	2	0.2350

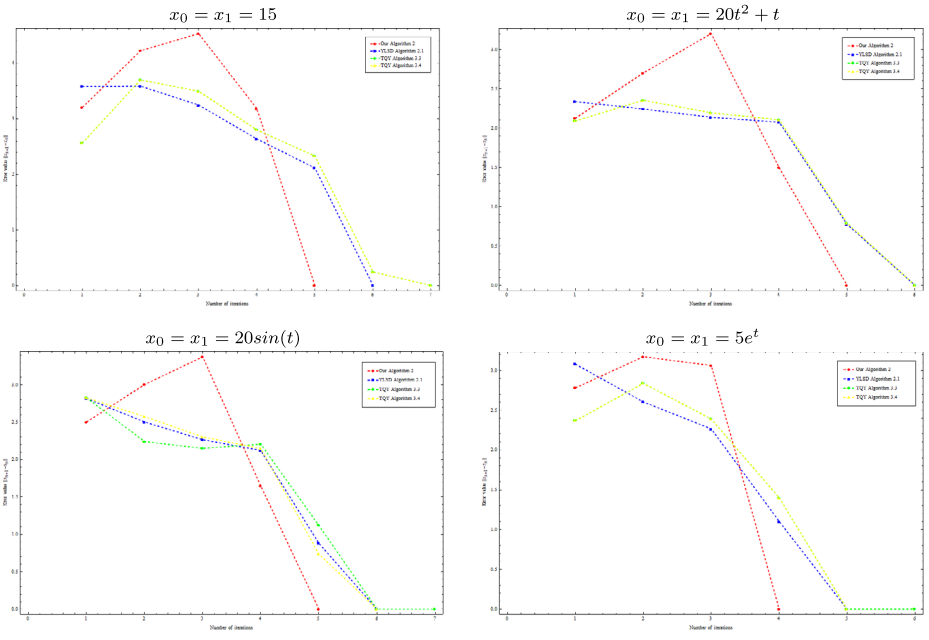

Figure 10 Convergence behaviors of the error sequences for $\psi_1 = \psi_2 = 1$

Remark 4.5 From the results in Tables 5, 6, and 7, we see that the quantities of loops n and the CPU times usage of all the compared algorithms depend on ψ_1 and ψ_2, which means that they are better for large ψ_1 and ψ_2, and worse for small ψ_1 and ψ_2, at the same time the speed of convergence behaves similarly. Moreover, the speed of convergence to the solution of the YLSD Algorithm 2.1 is better than others, their approximate solution function is $(x^*(t), y^*(t)) = (0., 0.)$, where "0." means that it is in interval $(-p, p)$, where $p = 2.22507 \times 10^{-308}$ (the smallest positive machine-precision number in MATHEMATICA), see Fig. 11.

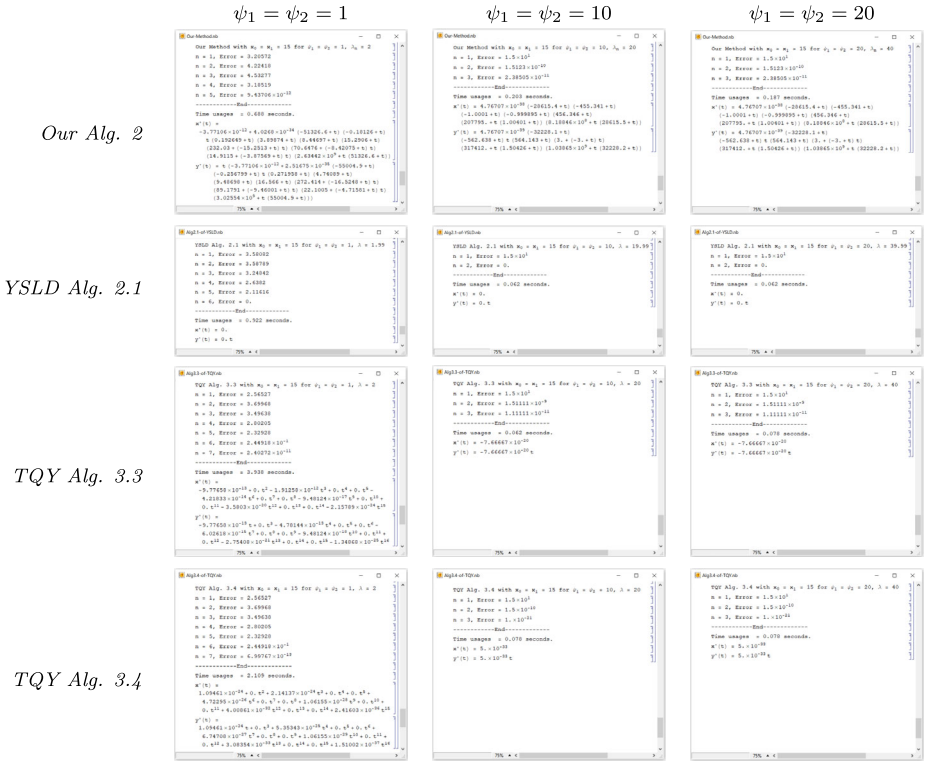

Figure 11 Approximate solution functions of Example 4.4 with initial functions $x_0(t) = x_1(t) = 15$

4.3 Convex minimization problem

Let $F_1 : H_1 \to \mathbb{R}$ be a convex and differentiable function and $G_1 : H_1 \to \mathbb{R} \cup \{\infty\}$ be a convex and lower semicontinuous function such that the gradient ∇F_1 is a $\frac{1}{\psi_1}$-Lipschitz continuous function and ∂G_1 is a subdifferential of G_1. If $F_2 = G_2 = 0$ then the SCMP is reduced to a convex minimization problem (CMP), which is to find $x^* \in H_1$ such that

$$F_1(x^*) + G_1(x^*) = \min_{x \in H_1}\{F_1(x) + G_1(x)\} \quad \Leftrightarrow \quad 0 \in \nabla F_1(x^*) + \partial G_1(x^*).$$

Example 4.6 We illustrate the performance of our Algorithm 3 in Theorem 4.1 for solving a convex minimization problem. We implemented them in MATHEMATICA 5.0 to solve and run on a personal laptop: Intel(R) Core(TM) i5-8250U CPU @1.80 GHz 8 GB RAM.

Find the minimization of the following ℓ_1-least-square problem:

$$\min_{x \in \mathbb{R}^3}\left\{\|x\|_1 + \frac{1}{2}\|x\|_2^2 - (2,3,4)x + 3\right\},$$

where $x = (u, v, w)^T \in \mathbb{R}^3$.

Let $H_1 = H_2 = (\mathbb{R}^3, \|\cdot\|_2)$, $F_1(x) = \frac{1}{2}\|x\|_2^2 - (2,3,4)x + 3$, $F_2(x) = 0$ and $G_1(x) = \|x\|_1$, $G_2(x) = 0$ for all $x \in \mathbb{R}^3$, and $A = I$. Then, $\nabla F_1(x) = (u-2, v-3, w-4)^T$ and $\nabla F_2(x) = (0,0,0)^T$ for all $x \in \mathbb{R}^3$. It follows that F_1 is convex and differentiable on $\mathbb{R}^3$ with $\psi_1 = 1$ of $\frac{1}{\psi_1}$-Lipschitz continuous gradient ∇F_1. Moreover, G_1 is convex and lower semicontinuous but not differentiable on $\mathbb{R}^3$.

Algorithm 3 The forward–backward algorithm with errors

procedure FBSA_Err3

Choose the initials $x_0, x_1 \in H_1$ arbitrarily. Set the error ϵ.

Set the mapping f in backing tracks.

$n \leftarrow 0$

repeat

$n \leftarrow n+1$

Update the parameters α_n, λ_n, θ_n and the error $\varepsilon_n \in H_1$.

$z_n \leftarrow x_n + \theta_n(x_n - x_{n-1})$

$y_n \leftarrow z_n$

$x_{n+1} \leftarrow \alpha_n f(y_n) + (1-\alpha_n)\operatorname{prox}_{\lambda_n G_1}((I - \lambda_n \nabla F_1)y_n + \varepsilon_n)$

until $\|x_{n+1} - x_n\| < \epsilon$

return x_{n+1}

end procedure

Table 8 Numerical results of Example 4.6 for the initial points $x_0 = (-1,2,1)^T$ and $x_1 = (2,-1,-2)^T$ using Algorithm 3 in Theorem 4.1

Type	λ_n for $L_1 = 1$	n	CPU (s)	x^*	$\|x_{n+1} - x_n\|_2$
A1	$\frac{L_1}{10}$	142	0.546	$(1.00001, 2.00000, 2.99999)^T$	8.78×10^{-7}
A2	$L_1 - \frac{L_1}{10}$	49	0.046	$(1.00001, 2.00001, 3.00001)^T$	9.60×10^{-7}
A3	L_1	48	0.047	$(1.00001, 2.00001, 3.00001)^T$	9.38×10^{-7}
A4	$L_1 + \frac{L_1}{10}$	47	0.063	$(1.00001, 2.00001, 3.00001)^T$	9.27×10^{-7}
A5	$2L_1 - \frac{L_1}{10}$	–	–	–	–
A6	$2L_1$	–	–	–	–
B1	$\frac{L_1 n}{n+1}$	48	0.046	$(1.00001, 2.00001, 3.00001)^T$	9.65×10^{-7}
B2	$\frac{L_1(n+2)}{n+1}$	47	0.046	$(1.00001, 2.00001, 3.00001)^T$	9.92×10^{-7}
B3	$\frac{2L_1 n}{n+1}$	–	–	–	–
C1	$L_1 + \frac{(-1)^n L_1}{n+1}$	37	0.031	$(1.00002, 2.00002, 3.00002)^T$	8.75×10^{-7}
C2	$L_1 + \frac{(-1)^{n+1} L_1}{n+1}$	36	0.031	$(1.00002, 2.00002, 3.00002)^T$	9.74×10^{-7}

We set $f(x) = \frac{x}{5}$ for all $x \in \mathbb{R}^3$. Then, f is a contraction. For each $n \in \mathbb{N}$, we choose $\alpha_n = \frac{10^{-6}}{n+1}$, $\varepsilon_n = \frac{1}{(n+1)^3}(1,1,1)^T$, $\xi_n = (0,0,0)^T$, and we define θ_n as (4.5), and for all $x \in \mathbb{R}^3$ we have

$$\begin{aligned}&\operatorname{prox}_{\lambda_n G_1}(x)\\ &\quad= \big(\operatorname{sign}(u)\max\{|u| - \lambda_n, 0\}, \operatorname{sign}(v)\max\{|v| - \lambda_n, 0\}, \operatorname{sign}(w)\max\{|w| - \lambda_n, 0\}\big)^T.\end{aligned}$$

We choose the initial points $x_0 = (-1,2,1)^T$ and $x_1 = (2,-1,-2)^T$ for computing the recursive of the sequence $\{x_n\}$ using Algorithm 3 in Theorem 4.1 with an error $\epsilon = 10^{-6}$ in each of the chosen types of the sequences $\{\lambda_n\}$ with $L_1 = \psi_1 = 1$ as in Table 8 (except for A5, A6, and B3 types because their convergence is slow). As $n \to \infty$, we obtain $x_n \to x^*$ such that the approximate minimization of $F_1 + G_1$ is $(1,2,3)^T$ and its approximate minimum value is -4, as in Table 8, and we also show the convergence behavior of the error sequences $\{\|x_{n+1} - x_n\|_2\}$ that converge to the zero value for each of the best choices A4, B2, and C2 types of the sequences $\{\lambda_n\}$, see Fig. 12.

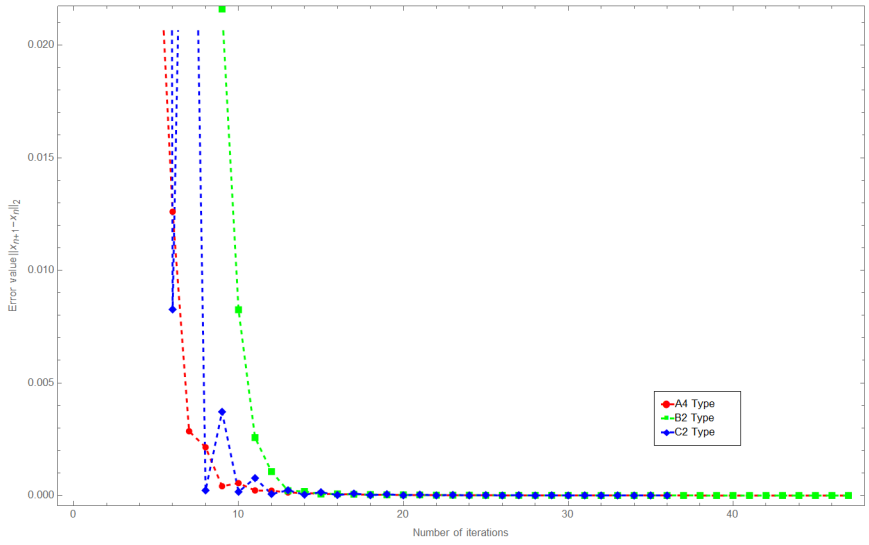

Figure 12 Convergence behavior of the error sequences $\{\|x_{n+1} - x_n\|_2\}$ for each of the best choices A4, B2, and C2 types in Example 4.6

Table 9 Choices of the parameter θ_n for testing the fast convergence with C2 type of the parameter λ_n

Choice	n	CPU (s)	x^*	$\|x_{n+1} - x_n\|_2$
1	34	0.016	$(1.00002, 2.00002, 3.00002)^T$	9.93×10^{-7}
2	34	0.016	$(1.00002, 2.00002, 3.00002)^T$	9.99×10^{-7}
3	34	0.015	$(1.00002, 2.00002, 3.00002)^T$	9.93×10^{-7}
4	36	0.031	$(1.00002, 2.00002, 3.00002)^T$	8.96×10^{-7}
5	36	0.031	$(1.00002, 2.00002, 3.00002)^T$	9.83×10^{-7}
6	36	0.031	$(1.00002, 2.00002, 3.00002)^T$	9.74×10^{-7}
7	36	0.016	$(1.00002, 2.00002, 3.00002)^T$	8.96×10^{-7}

We next consider seven different choices of the parameter θ_n for testing the fast convergence as (4.6) and (4.7) with C2 type of the parameter λ_n only, and the others as they were.

From the results of the seven different choices of the parameter θ_n as in Table 9, we see that the quantities of loops n and the CPU times usage of choices 1, 2, and 3 are less than the others, and we conclude that choices 1, 2, and 3 of the parameter θ_n are to be an accelerated choice for the speed up of convergence of solving this simple example.

5 Conclusion

A new iterative forward–backward splitting algorithm with errors (FBSA_Err) for solving SMVIP is obtained in our main result. It can be applied to solving the image-feature extraction with multiple-image blends problem. Under the encrypted image $L = A * H$, which is generated by the linear method of element-wise multiplication of A and H such that stacking the columns of $A \in \mathbb{R}^{m\times m}$ corresponding with the discrete logistic chaotic map $\{x_n\}_{n=1}^{m^2}$, and setting all parameters to their fast convergence, we obtain the following results:

1. For the quality measure of the decrypted image by the NCC measure only, A1, A6, and A6 types of the parameters γ_n, λ_n, and η_n, respectively, and choice 6 of the

parameter θ_n as (4.5) are the best choices to solve the image-feature extraction with multiple-image blends problem using FBSA_Err.

2. For the quality measure of the decrypted image by NCC, SNR, and ISNR measures together, A2, A6, and A6 types of the parameters γ_n, λ_n, and η_n, respectively, and choice 6 of the parameter θ_n as (4.5) are the best choices to solve the image-feature extraction with multiple-image blends problem using FBSA_Err.

For application of our main result to the split variational inclusion problem or the split minimization problem, compared with the YSLD Algorithm 2.1 [43], TQY Algorithms 3.3 and 3.4 [44], and the TDC Algorithm 3.3 [45], the speed of convergence to the solution of the YLSD Algorithm 2.1 is better than the others except for complex problems (e.g., the image/signal-recovery problems).

For application of our main result to the convex minimization problem, theC2 type of the parameter λ_n and choices 1, 2, and 3 of the parameter θ_n are the best choices to solve the convex minimization problem.

Acknowledgements
The author would like to thank the Editor and anonymous referees for comments and remarks that improved the quality and presentation of the paper, and the Faculty of Science, Maejo University for its financial support.

Funding
This research was supported by the Faculty of Science, Maejo University.

Availability of data and materials
Not applicable.

Declarations

Ethics approval and consent to participate
Not applicable.

Consent for publication
Not applicable.

Competing interests
The authors declare no competing interests.

Author contributions
All authors contributed equally to the writing of this paper. All authors read and approved the final manuscript.

Received: 25 December 2021 Accepted: 12 April 2023 Published online: 01 May 2023

References

1. Bauschke, H.H.: The approximation of fixed points of compositions of nonexpansive mappings in Hilbert space. J. Math. Anal. Appl. **202**, 150–159 (1996)
2. Chidume, C.E., Bashir, A.: Convergence of path and iterative method for families of nonexpansive mappings. Appl. Anal. **67**, 117–129 (2008)
3. Halpern, B.: Fixed points of nonexpansive maps. Bull. Am. Math. Soc. **73**, 957–961 (1967)
4. Ishikawa, S.: Fixed points by a new iteration method. Proc. Am. Math. Soc. **44**, 147–150 (1974)
5. Klen, R., Manojlovic, V., Simic, S., Vuorinen, M.: Bernoulli inequality and hypergeometric functions. Proc. Am. Math. Soc. **142**, 559–573 (2014)
6. Kunze, H., La Torre, D., Mendivil, F., Vrscay, E.R.: Generalized fractal *n* transforms and self-similar objects in cone metric spaces. Comput. Math. Appl. **64**, 1761–1769 (2012)
7. Mann, W.R.: Mean value methods in iteration. Proc. Am. Math. Soc. **4**, 506–510 (1953)
8. Radenovic, S., Rhoades, B.E.: Fixed point theorem for two non-self mappings in cone metric spaces. Comput. Math. Appl. **57**, 1701–1707 (2009)
9. Todorcevic, V.: Harmonic Quasiconformal Mappings and Hyperbolic Type Metrics. Springer, Basel (2019)
10. Byrne, C.: Iterative oblique projection onto convex subsets and the split feasibility problem. Inverse Probl. **18**, 441–453 (2002)
11. Byrne, C.: A unified treatment of some iterative algorithms in signal processing and image reconstruction. Inverse Probl. **20**, 103–120 (2004)
12. Combettes, P.L., Wajs, V.: Signal recovery by proximal forward-backward splitting. Multiscale Model. Simul. **4**, 1168–1200 (2005)

13. Censor, Y., Bortfeld, T., Martin, B., Trofimov, A.: A unified approach for inversion problems in intensity-modulated radiation therapy. Phys. Med. Biol. **51**, 2353–2365 (2006)
14. Censor, Y., Elfving, T., Kopf, N., Bortfeld, T.: The multiple set split feasibility problem and its applications. Inverse Probl. **21**, 2071–2084 (2005)
15. Censor, Y., Motova, A., Segal, A.: Perturbed projections and subgradient projections for the multiple-sets feasibility problem. J. Math. Anal. **327**, 1244–1256 (2007)
16. Moudafi, A.: Split monotone variational inclusions. Adv. Differ. Equ. **150**, 275–283 (2011)
17. Nimana, N., Petrot, N.: Viscosity approximation methods for split variational inclusion and fixed point problems in Hilbert spaces. In: Proceedings of the International MultiConference of Engineers and Computer Scientists, vol. 2 (2014)
18. Che, H., Li, M.: Solving split variational inclusion problem and fixed point problem for nonexpansive semigroup without prior knowledge of operator norms. Math. Probl. Eng. **2015**, Article ID 408165 (2015)
19. Shehu, Y., Ogbusi, F.U.: An iterative method for solving split monotone variational inclusion and fixed point problems. Rev. R. Acad. Cienc. Exactas Fís. Nat., Ser. A Mat. **110**, 503–518 (2016)
20. Thong, D.V., Cholamjiak, P.: Strong convergence of a forward-backward splitting method with a new step size for solving monotone inclusions. Comput. Appl. Math. **38**, 94 (2019)
21. Alansari, M., Farid, M., Ali, R.: An iterative scheme for split monotone variational inclusion, variational inequality and fixed point problems. Adv. Differ. Equ. **2020**, 485 (2020)
22. Ogbuisi, F.U., Mewomo, O.T.: Solving split monotone variational inclusion problem and fixed point problem for certain multivalued maps in Hilbert spaces. Thai J. Math. **19**(2), 503–520 (2021)
23. Alakoya, T.O., Mewomo, O.T.: Viscosity S-iteration method with inertial technique and self-adaptive step size for split variational inclusion, equilibrium and fixed point problems. Comput. Appl. Math. **41**(1), 39 (2022)
24. Ogwo, G.N., Alakoya, T.O., Mewomo, O.T.: Inertial iterative method with self-adaptive step size for finite family of split monotone variational inclusion and fixed point problems in Banach spaces. Demonstr. Math. **55**(1), 193–216 (2022)
25. Godwin, E.C., Alakoya, A., Mewomo, O.T., Yao, J.C.: Relaxed inertial Tseng extragradient method for variational inequality and fixed point problems. Appl. Anal. (2022). https://doi.org/10.1080/00036811.2022.2107913
26. Godwin, E.C., Izuchukwu, C., Mewomo, O.T.: Image restoration using a modified relaxed inertial method for generalized split feasibility problems. Math. Methods Appl. Sci. (2022). https://doi.org/10.1002/mma.8849
27. Alakoya, T.O., Uzor, V.A., Mewomo, O.T., Yao, J.C.: On a system of monotone variational inclusion problems with fixed-point constraint. J. Inequal. Appl. **2022**, 47 (2022)
28. Alakoya, T.O., Uzor, V.A., Mewomo, O.T.: A new projection and contraction method for solving split monotone variational inclusion, pseudomonotone variational inequality, and common fixed point problems. Comput. Appl. Math. (2022). https://doi.org/10.1007/s40314-022-02138-0
29. Tianchai, P.: The zeros of monotone operators for the variational inclusion problem in Hilbert spaces. J. Inequal. Appl. **2021**, 126 (2021)
30. Tianchai, P.: An improved fast iterative shrinkage thresholding algorithm with an error for image deblurring problem. Fixed Point Theory Algorithms Sci. Eng. **2021**, 18 (2021)
31. Takahashi, W.: Introduction to Nonlinear and Convex Analysis. Yokohama Publ., Yokohama (2009)
32. Tang, J.F., Chang, S.S., Yuan, F.: A strong convergence theorem for equilibrium problems and split feasibility problems in Hilbert spaces. Fixed Point Theory Appl. **2014**, 36 (2014)
33. Nadezhkina, N., Takahashi, W.: Weak convergence theorem by an extragradient method for nonexpansive mappings and monotone mappings. J. Optim. Theory Appl. **128**, 191–201 (2006)
34. Geobel, K., Kirk, W.A.: Topic in Metric Fixed Point Theory. Cambridge Studies in Advanced Mathematics, vol. 28. Cambridge University Press, Cambridge (1990)
35. Nakajo, K., Shimoji, K., Takahashi, W.: Strong convergence to common fixed points of families of nonexpansive mappings in Banach spaces. J. Nonlinear Convex Anal. **8**(1), 11–34 (2007)
36. Takahashi, W., Takeuchi, Y., Kubota, R.: Strong convergence theorems by hybrid methods for families of nonexpansive mappings in Hilbert spaces. J. Math. Anal. Appl. **341**, 276–286 (2008)
37. Takahashi, W., Xu, H.-K.: Iterative algorithms for nonlinear operators. J. Lond. Math. Soc. **66**, 240–256 (2002)
38. He, S., Yang, C.: Solving the variational inequality problem defined on intersection of finite level sets. Abstr. Appl. Anal. **2013**, Article ID 942315 (2013)
39. Baillon, J.B., Haddad, G.: Quelques proprietes des operateurs angle-bornes et cycliquement monotones. Isr. J. Math. **26**, 137–150 (1977)
40. Rockafellar, R.T.: On the maximal monotonicity of subdifferential mappings. Pac. J. Math. **33**, 209–216 (1970)
41. Image Databases: Available online: http://www.imageprocessingplace.com/downloads_V3/root_downloads/image_databases/standard_test_images.zip. Accessed 1 Sept 2021
42. Can Stock Photo: Available online: https://www.canstockphoto.com/help-message-in-a-bottle-25858836.html. Accessed 1 Sept 2021
43. Yao, Y., Shehu, Y., Li, X.H., Dong, Q.L.: A method with inertial extrapolation step for split monotone inclusion problems. Optimization **70**(4), 741–761 (2021)
44. Tan, B., Qin, X., Yao, J.C.: Strong convergence of self-adaptive inertial algorithms for solving split variational inclusion problems with applications. J. Sci. Comput. **87**, 20 (2021)
45. Thong, D.V., Dung, V.T., Cho, Y.J.: A new strong convergence for solving split variational inclusion problems. Numer. Algorithms **86**, 565–591 (2021)
46. Bauschke, H.H., Combettes, P.L.: Convex Analysis and Monotone Operator Theory in Hilbert Spaces, 2nd edn. Springer, New York (2017)

Publisher's Note